RAPID DETERMINATION OF EARTHQUAKE MAGNITUDE USING ElarmS

by

Zeynep Coşkun

B.S., Geophysical Engineering, Sakarya University, 2006

Submitted to the Kandilli Observatory and

Earthquake Research Institute

in partial fulfillment of the requirements for the degree of

Master of Science

Graduate Program in Geophysics

Boğaziçi University

2010

RAPID DETERMINATION OF EARTHQUAKE MAGNITUDE USING ElarmS

APPROVED BY:

Prof. Mustafa Aktar   ……………………..
(Thesis Supervisor)

Assoc. Prof. Serdar Özalaybey   ……………………..
(Thesis Co-advisor)
(TÜBİTAK)

Prof. Hayrullah Karabulut   ……………………..

Prof. Oğuz Özel
(İstanbul University)   ……………………..

DATE OF APPROVAL: 16.06.2010

ACKNOWLEDGEMENTS

I am heartily thankful to my supervisor, Prof. Mustafa Aktar, for his invaluable encouragement, support and guidance during the preparation of my master thesis. I would like to express my sincere gratitude to him for his great ideas and endless patience. I have learned not only scientific information from him, but also how to identify a problem, how to overcome difficulties and how to reach results. I would also like to thank my Co-advisor, Assoc. Prof. Serdar Özalaybey, for his contributions during the preparation of my master thesis.

I am grateful to all faculty members in Geophysics Department for their support and contributions.

I have benefited from National Earthquake Monitoring Center during my thesis. I would like to thank all the staff at NEMC.

I would like to thank my dear friends: Gülçin Güner, Leyla Aslı Er and Res. Assist. Öcal Necmioğlu for their great support and help. Working with them was so joyful, I thank them all. I am also thankful to Res. Assist. Yaman Özakın and Res. Assist. Birsen Can who spent their invaluable time with me.

I owe my deepest gratitude to my parents; I have no words to express how much I owe to my dad Halil Coşkun, my mom Ayten Coşkun and my dear sister İpek Coşkun.

ABSTRACT

RAPID DETERMINATION OF EARTHQUAKE MAGNITUDE USING ElarmS

Earthquake Alarms Systems, ElarmS, is designed with the goal of providing warning of forthcoming ground shaking during earthquakes. The event magnitude is found to scale with the maximum predominant period, $\tau_p^{\ max}$, which is estimated, using the frequency content of the first few seconds of the P-wave arrival from the vertical component of velocity records. I tested ElarmS offline using 242 earthquakes with magnitudes between 0.5 and 5.1 occurred across The Gulf of Gökova, Turkey. The test data for small magnitude events were obtained from the detailed re-processing of August 2007 with additional data from temporary stations. The larger events were directly taken from NEMC catalogue. I found that events smaller than 3.0 did not have clear relation between $\tau_p^{\ max}$ and event magnitude, on the other hand, events with magnitude larger than 3.0 showed a scaling relation between $\tau_p^{\ max}$ and event magnitude. The relation obtained for Gokova was consistent with the ones obtained in California and Japan. The average magnitude error between real local magnitude and ElarmS magnitude was about $\pm$ 0.91 magnitude units when single closest station to the epicenter was used. Once data from the two closest stations available the error drops to $\pm$ 0.62, when six station data available the error drops to $\pm$ 0.49.

ÖZET

ElarmS YÖNTEMİ KULLANILARAK DEPREM MAGNİTÜDÜNÜN HIZLI TAYİNİ

Deprem Alarm Sistemi, ElarmS, depremler sırasında yaklaşan yer sarsıntısı için uyarı vermek amacıyla tasarlanmıştır. Hız kayıtlarının düşey bileşeninden, P dalga varışının ilk birkaç saniyesindeki frekans içeriğini kullanarak, en yüksek hakim periyot, τ_p^{max}, depremin büyüklüğüyle ölçeklenmek için bulunur. ElarmS'ı offline, büyüklükleri 0.5 ve 5.1 arasında değişen Gökova Körfezi, Türkiye çevresinde olmuş 242 depremle test ettim. Küçük magnitüdlü deprem verilerini Ağustos 2007 ve geçici istasyon verilerinin detaylı olarak incelenmesiyle elde ettim. Daha büyük depremleri ise direkt Ulusal Deprem İzleme Merkezi'nin kataloğundan aldım. 3.0 dan küçük depremler için τ_p^{max} ve büyüklük arasında ilişki bulamadım, öte yandan 3.0 dan büyük depremler için τ_p^{max} ve büyüklük arasında ölçeklenir ilişki buldum. Gökova için bulduğum bu ilişki California ve Japonya ile uyum gösterdi. Gerçek lokal büyüklük ve ElarmS'la hesaplanan büyüklük arasındaki ortalama büyüklük hatası deprem merkezine en yakın tek istasyon kullanıldığında ± 0.91 civarındaydı. İki yakın istasyon verisi mevcut olduğu zaman hata ± 0.62, altı istasyon verisi mevcut olduğu zaman hata ± 0. 49 a düştü.

TABLE OF CONTENTS

LIST OF FIGURES

LIST OF TABLES

LIST OF SYMBOLS / ABBREVIATIONS

D_i	Smoothed velocity derivatived squared at time i
Mb	Body wave magnitude
Mc	Completeness threshold
Me	Equivalent magnitude
Ml	Local magnitude
Mw	Moment magnitude
Pd	Peak displacement
X_i	Smoothed ground velocity squared at time i
x_i	Ground velocity recorded at time i
α	Smoothing constant
τ_p	Predominant period
$\tau_p^{\ max}$	Maximum predominat period
$\tau_i^{\ p}$	Predominant period for sample i
π	Pi
A.D	Anno Domini
amp	Amplitude
ANNs	Artificial neural networks
B.C	Before Christ
BLCB	Balçova station
BODT	Bodrum station
BU	Boğaziçi University
CETI	Çetibeli station

CISN	California Integrated Seismic Network
CWB	The Taiwan Central Weather Bureau
DALT	Dalaman station
DAT	Datça station
DIST	Distance
EEWS	Earthquake early warning systems
ElarmS	Earthquake Alarms Systems
ELL	Elmalı station
E-W	East-West
FETY	Fethiye station
GPS	Global positioning system
HYPO	Hypocenter
Hz	Hertz
INSN	The new Italian National Seismic Network
ISK	İstanbul Kandilli Station
ISNet	The Irpinia Seismic Network
Lat	Latitude
log	Logarithm
Lon	Longitude
K-Net	Kyoshin Net
KOERI	Kandilli Observatory and Earthquake Research Institute
MLSB	Milas station
NEMC	National Earthquake Monitoring Center
N-S	North-South
OZCA	Özcan station

PQL	PASSCAL Quick Look
PreSEIS	Pre-seismic shaking
RTD	Rapid Earthquake Information Release System
SAC	Seismic Analysis Code
SAS	The Seismic Alarm System
SAS	The Seismic Alert System
SNR	Signal to noise ratio
STNM	Station name
TURG	Turgutlu station
UrEDAS	Urgent Earthquake Detection and Alarm System
VSN	Virtual Subnetwork
Vz	Vertical component of velocity record
YER	Yerkesik station

1. INTRODUCTION

Turkey is located at the junction of the Eurasian, Arabian and African plates, and transected by diverse active plate boundaries. Geologically, Turkey is a part of the great Alpine belt which widen from the Atlantic Ocean to the Himalayas, in consequence, Turkey is one of the most seismically active region in the world (USGS, 1995). Unfortunately, this activity caused serious damages and loss of lives over both historical and modern times. Magnitude of earthquakes in Turkey ranges from small tremors to larger ones. For example two damaging earthquakes occurred on 17 August 1999 Mw 7.4 in İzmit and on 12 November 1999 Mw 7.2 in Düzce. İzmit and Düzce earthquakes caused 18.373 accounted deaths, 48.901 injuries, 16.400 heavily damaged and collapsed buildings, and 600.000 homeless people (Erdik, 2000). Even moderate size events can cause large-scale damage to buildings that are constructed poorly, especially over rural areas. For example on 18 March 2010 Başyurt-Karakoçan, Elazığ earthquake Ml 6.0 occurred which caused 42 deaths, 137 injuries and 8422 damaged buildings (Kalafat *et al*., 2010). This damage potential caused by earthquakes in Turkey will continue to exist and cause more damages as the population grows. At this point, the importance of the Earthquake Early Warning System rises.

The goal of the Earthquake Early Warning Systems (EEWS) is to detect the earthquake close to the epicenter and issue warning of the forthcoming ground shaking to the authorities and public. Such systems are in operation in Mexico, Taiwan and Japan (Allen and Kanamori, 2003). For example, in 1995 in Mexico City EEWS succeeded in issuing alarm to the public 72 sec ahead of strong ground shaking generated by an earthquake with magnitude 7.4 originating from Guerrero Gap, located at a distance of ~300 km of the city (Allen and Kanamori, 2003). The system in Mexico uses front detection which detects earthquakes close to the epicenter, determine magnitude and issue warning using radio broadcast (Allen and Kanamori, 2003). An Early Warning System is also in operation for the city of Istanbul aimed at detecting large events expected to occur on the Marmara Faults (Böse *et al*., 2007). In this case, the problem is more challenging because the active faults are very close to the metropolitan areas and the warning time is relatively very short. In actual system front detection approach is implemented. New and

more involved methods using neural network approaches are under development (Böse *et al*., 2007). It is clear that efficient and reliable methods are needed to estimate the magnitude from the very first seconds of the incoming wave and make the Early Warning System more effective.

In this study I tested Earthquake Alarm Systems, ElarmS, which uses P-arrival that are detected by seismic stations at the epicentral region and determine the magnitude of the earthquake (Allen and Kanamori, 2003). The approach aims to issue a warning even when the first waves arrive to few stations closest to the epicenter, in other word before the beginning of the strong ground shaking which mostly come later with the S and surface waves (Allen and Kanamori, 2003).

I tested ElarmS around the Gulf of Gökova (Turkey) which is one of the most seismically active places of southwest Anatolia. It is known that throughout history the region was affected by large destructive earthquakes and the activity is still continuing intensely in the last decades. In recent years, many broadband stations of both permanent and temporary status were installed around the Gökova Gulf. A wide range of magnitudes were recorded at close distances and collections of large number of high quality digital seismograms are already available. This constitutes one of the main reasons for choosing the area for this pilot study. Furthermore, since earlier studies on ElarmS method was mostly based on strike-slip fault mechanisms, the choice of Gökova is expected to provide the first example for the normal fault regime. Finally, since the region is experiencing a rapid growth of population especially in summer months, the earthquake hazard due to strong ground motion as well as tsunami generation is becoming an important issue. An Early Warning System will definitely be a tool that will need be considered in the future not only for settlements but also the large power plants that are located in the area.

I have investigated the state-of-art implementations of EEWS around the world in Chapter 2, and have given two examples about two offline ElarmS tests that were performed in Italy and Japan. Chapter 3 includes brief information about the tectonic regime of the study area in particular recent studies that try to locate the main fault structures off-shore. In Chapter 4, I have compiled all destructive historical events from B.C 412 to the recent ones with magnitudes larger than four. In Chapter 5, I have

processed the August 2007 data and have compared them with NEMC's catalogue. The Methodology of the ElarmS system has been explained in detail in Chapter 6 and also the application of the system around the study area has been illustrated in this chapter. Due to inability of the ElarmS algorithm for some of the events, I have tested the system with using synthetic data and have given the results of this test in Chapter 6 too. Finally, Chapter 7 give a summary of the highlights of the study, relate them to the general theoretical background and outline the final concluding remark.

2. OVERVIEW OF EARTHQUAKE EARLY WARNING SYSTEMS (EEWS)

In general terms, earthquake early warning is the quick determination of an earthquake before its arrival to urban areas, and provision warning to people. The importance of the term "early warning" has been growing especially for the past few decades due to the fact that as population in large cities grows faster people face with a greater risk and these natural disasters caused thousands of loss of lives and economic losses.

The length of warning time depends on the distance from the earthquake epicenter to urban areas (Allen, 2009). Depending on the space between active fault zones to metropolitan areas, the warning time can vary from a few seconds to a few tens of seconds before the damaging ground shaking arrives (Allen and Kanamori, 2003).

The operation of earthquake early warning systems bring great benefits with respect to reduce damage of major engineered systems such as nuclear power plants, lifelines or transportation systems, and also let people secure themselves when they are alerted (Gasparini *et al*., 2007).

The implementations of EEWS have been rapidly spreading around the world, and in Japan, Taiwan, Mexico, Turkey and Romania, warning systems are currently in use (Allen, 2010a). Figure 2.1 shows the regions where earthquake early warning systems are in operation (Allen, 2010b).
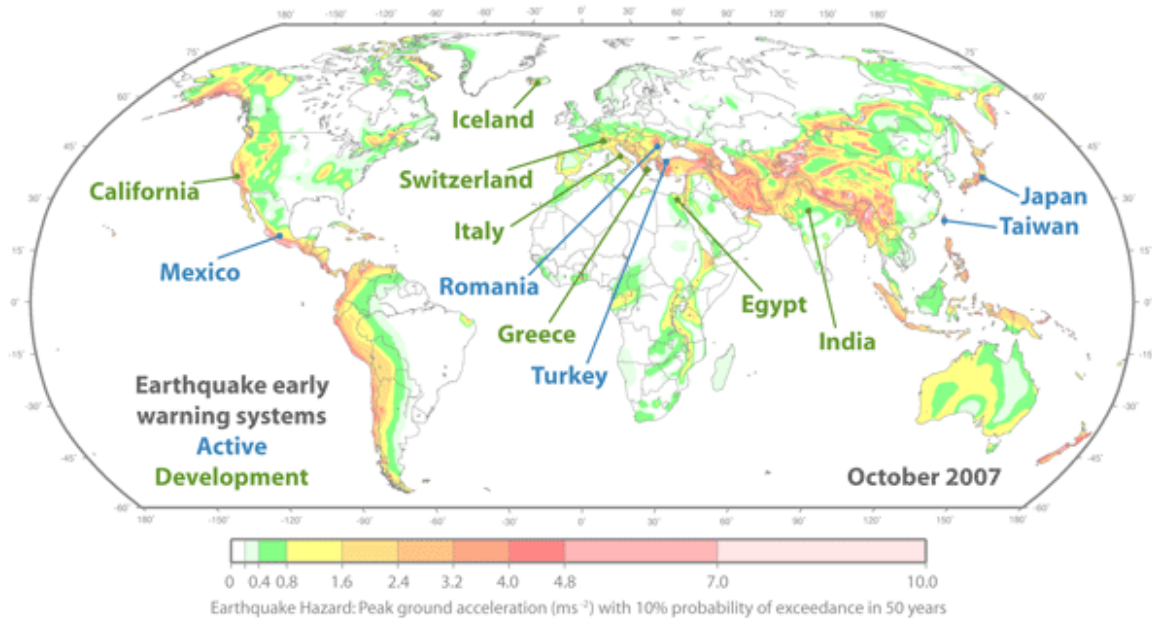
Figure 2.1. The global hazard map shows regions active EEWS in blue and developing in green (Allen, 2010b)

2.1. Earthquake Early Warning Systems in Operation

In Japan, early in the 1950s, alarm seismometers were installed along railways in order to cut power when the seismometers detect ground motion pass beyond some threshold along the tracks (Nakamura and Tucker, 1988). During the 1980s Urgent Earthquake Detection and Alarm System, UrEDAS, replaced them (Allen and Kanamori, 2003). UrEDAS is the first real time P-wave alarm system to be operative in the world, which determines earthquake magnitude and location (Nakamura, 1988). There are two types of UrEDAS: UrEDAS and Compact UrEDAS (Nakamura, 2004). UrEDAS is utilized to estimate magnitude and location of earthquake by P-wave and issue warning to places under risk, besides Compact UrEDAS is used to evaluate whether the earthquake is going to be destructive or not, and additionally issue an alarm when needed (Nakamura, 2004).

In Mexico, The Seismic Alert System, SAS, was deployed to provide warning in Mexico City of earthquakes which are derived from the subduction zone of Pacific coast at a distance of about 320 km (Gasparini *et al*., 2007). The system provides warning time

varies between 58 and 74 sec (Gasparini *et al*., 2007). The function of the system is to receive information from the stations, automatically process the data, determine the magnitude of the earthquake, and make decision to issue a public alert or not (Allen and Kanamori, 2003). The warning is issued in two ways: The Radio Warning System issues warning via commercial radio stations and other audio alerting mechanisms warn the residents of Mexico City, public schools, public transportation systems, government, some industries and other key utilities (Allen and Kanamori, 2003).

In Taiwan, since 1995, The Taiwan Central Weather Bureau, CWB, has utilized its Rapid Earthquake Information Release System, RTD, by applying a Virtual Subnetwork, VSN (Wu and Teng, 2002). VSN system is a regional system which uses a real-time, 97 telemetred strong motion signals across Taiwan and it is able to reduce the earthquake reporting time to about 30 sec or less with an average of about 22 sec from the origin (Wu and Teng, 2002). If the nucleation point is located less than 70 km from a settlement then the system is not useful, but the lead time increases more than 10 sec when the distance is greater than 100 km from the earthquake source (Wu and Teng, 2002).

In Romania, the system performed was designed to protect especially Bucharest and some industrial structures from the intermediate depths between 60 km and 200 km earthquakes originating in the Vrancea region which is located at the sharp bend of the Eastern Carpathian Arc (Ionescu *et al*., 2007). The system is low-cost, robust and allows roundly 25 sec time window for Bucharest (Ionescu *et al*., 2007).

In Turkey, the mega-city Istanbul is under high-seismic risk owing to western continuation of the North Anatolian Fault Zone, the Main Marmara Fault (Böse *et al*., 2007). Unfortunately, the distance of the segments of the fault to the coast of the Sea of Marmara and Istanbul is only about 20 kilometers (Böse *et al*., 2007). Due to this reason, a new approach was developed for EEWS that takes the advantage of both on-site warnings with single stations and network based regional strategies (Böse *et al*., 2007). Pre-seismic shaking, PreSEIS, method is fast as on-site warnings moreover gathers information from several stations with gaps of about 100 km to estimate source parameters of earthquakes from the first few seconds of the seismic signals (Böse *et al*., 2007). PreSEIS method is based on artificial neural networks, ANNs, in order to estimate the magnitude, source and

rupture locations of earthquakes (Böse *et al*., 2007).

In California, the region is dissected by many active faults and some of them are beneath the metropolitan areas (Allen and Kanamori, 2003). For this reason, it was aimed to issue a warning from the beginning of the strong ground motion, even at the epicenter (Allen and Kanamori, 2003). Therefore Earthquake Alarms Systems, ElarmS, was developed to estimate the size of the earthquake using the detected P arrival at the stations in the epicentral region (Allen and Kanamori, 2003). The system uses the frequency content of the first arriving pulse at the surface to estimate the magnitude, arrival times to define the location of the event, and finally generate a predicted ShakeMap, AlertMap, using a radial attenuation relation (Allen, 2007).

In Italy, The Irpinia Seismic Network, ISNet, was designed in 2002 as an advanced research seismic network, with the goal of protecting public buildings and infrastructure of strategic importance (Weber *et al*., 2007). In order to obtain highly dynamic recording range, each station was equipped with a strong-motion accelerometer and a velocitymeter (Weber *et al*., 2007). The system has been implemented in the southern Apennine chain, southern Italy, which is responsible of many strong crustal earthquakes in previous centuries (Weber *et al*., 2007). ISNet local network was developed together with the Civil Protection of the Campania Regional Authority and publish the signals to the Naples (Gasparini *et al*., 2007).

In Lithuania, the seismic alarm system, SAS, was designed with the goal of protecting Ignalia nuclear power plant from potentially damaging earthquakes by issuing an alarm before the arrival of the shear waves to the reactor (Gasparini *et al*., 2007). As a seismic "fence", 30 km from the power plant with constituting an array, totally six SAS stations were installed (Gasparini *et al*., 2007). According to the test results, when an earthquake with an epicenter outside the fence was occurred, that event was detected approximately four seconds before it was felt by the reactor (Gasparini *et al*., 2007). It was mentioned that two seconds were required to insert control rods (Gasparini *et al*., 2007). As a result, there is a chance to shut down the reactor before the strong ground shaking arrives (Gasparini *et al*., 2007).

In this study we tested Earthquake Alarms System, ElarmS, offline data from Gökova region, Turkey. ElarmS was designed with the goal of providing warning in California and other earthquake risky areas around the world (Allen, 2010a). The system is being tested in California by using real time data by California Integrated Seismic Network, CISN, and also has been tested by using offline data in Japan, Taiwan, Italy, Alaska, the Pacific Northwest and California (Allen, 2010a).

2.2. The ElarmS Earthquake Early Warning System

Earthquake Alarm Systems is a method which provides warning of forthcoming ground shaking during earthquakes (Allen, 2007). The method based on detecting the first arriving energy at the surface by using seismic instruments in a network and translating the information, which these low amplitude waves contain, first into an estimation of the earthquake size and then into a prediction of the peak ground shaking (Allen, 2007). The instruments that are adjacent to the epicenter detect the P-wave first, and this information can be integrated to produce a ground shaking map everywhere by using a seismic network (Allen, 2007). The ElarmS methodology uses the frequency content and arrival times of the P-wave in order to estimate earthquake magnitude and location respectively and finally predicts the ground shaking using a radial attenuation relation (Allen, 2007). All data coming from the seismic instruments is gathered regularly and the hazard map updated every second (Allen, 2007).

The methodology of the ElarmS is going to be explained in the following chapters in detail. Primarily we are going to exemplify two offline ElarmS tests that were performed in Italy and Japan.

2.2.1. The ElarmS Application across Italy

Italy has faced with seven destructive earthquakes with magnitudes greater than 6.0 in the past century (Olivieri *et al*., 2008). In order to monitor Italian seismicity, a network, the New Italian National Seismic Network, INSN, was deployed that consists 250 broadband stations with a typical spacing of approximately 40 km (Olivieri *et al*., 2008). The ElarmS methodology was tested offline on a data set of 225 earthquakes with

magnitudes between 2.5 and 6.0 (Olivieri *et al*., 2008). A scaling relation for determining the magnitude of an earthquake from the predominant period of the first few seconds of the signal was developed from the data set (Olivieri *et al*., 2008). As a result, it was found that the standard deviation in the error of the estimated magnitude was 0.4 magnitude units, when the maximum error in the data set didn't pass beyond +/- 0.75 (Olivieri *et al*., 2008).

2.2.2. The ElarmS Application across Japan

ElarmS method was tested in Japan in order to control the robustness of the system in completely different geologic region (Brown and Allen, 2009). The Japanese test dataset consists of 84 earthquakes with magnitudes range from 4.0 to 8.0 (Brown and Allen, 2009). 43 of them were 6.0 or greater (Brown and Allen, 2009). The earthquakes were recorded by Japan's Kyoshin Net, K-Net, strong-motion seismic network which contains 1000 digital strong-motion seismometers scattered across Japan with nearly 25 km spacing (Brown and Allen, 2009). Apart from determining the relation between predominant period and magnitude, peak displacement, P_d, is also read from the data in order to scale with event magnitude (Brown and Allen, 2009). Both scaling parameters, P_d and τ_p^{max} were effective at estimating final magnitude of the event from the first few seconds of the P wave (Brown and Allen, 2009). As a result, scaling relations showed that using one station the average error is approximately 0.75 magnitude units, dropping to 0.65 with two stations and 0.45 once four stations provide data (Brown and Allen, 2009).

3. OVERVIEW OF THE GULF OF GÖKOVA REGION

The Gulf of Gökova region is located at the southwest Anatolia – southeast Aegean Sea, Turkey. The study region is surrounded by Datça Peninsula from the south, Bodrum peninsula from the north and the island of Kos from the west (Uluğ and Kaşer, 2007).

The first observation in the region was made by Philippson at Datça Peninsula in 1915 (Ersoy, 1991). Ercan *et al.,* (1982) investigated especially the Neogen volcanizm and sediments of the region (Ersoy, 1991). Dewey and Şengör (1987), Le Pichon and Angelier (1991), Seyitoğlu and Scott (1991) mentioned that the gulf is under a north-south regional extensional tectonic system, producing structures such as Simav, Gediz and Büyük Menderes Grabens (Aktar *et al*., 2006). Ersoy (1991) investigated the expansion and the relation of Toros Nappes and ophiolites (Aktar *et al*., 2006). According to Görür *et al.,* (1995), the evolution of the rift formation in Gökova region has followed two different stages (Aktar *et al*., 2006). The present evolution was determined with N-S trending extension, and as a result the E-W trending grabens were formed in the region (Aktar *et al*., 2006). Figure 3.1 shows the overlapping rift and graben systems (Uluğ *et al*., 2005).

The first study about the fault system of the gulf was carried out by Barka (1985) for site selection of the Gökova Thermoelectric Power Plant (Aktar *et al*., 2006). That study pointed out the presence of a normal fault following the north shore of the gulf, and emphasized that the fault continues offshore to the west towards the Island of Kos, and to the east towards Ula-Yerkesik-Gökova direction (Aktar *et al*., 2006). The total length of the fault was determined as 180 km, and the Gulf of Gökova was described as half graben (Aktar *et al*., 2006). On the other hand, Ersoy (1991) argued that the Gökova Graben was bounded with two faults following the northern and the southern shore of the gulf (Ersoy, 1991).
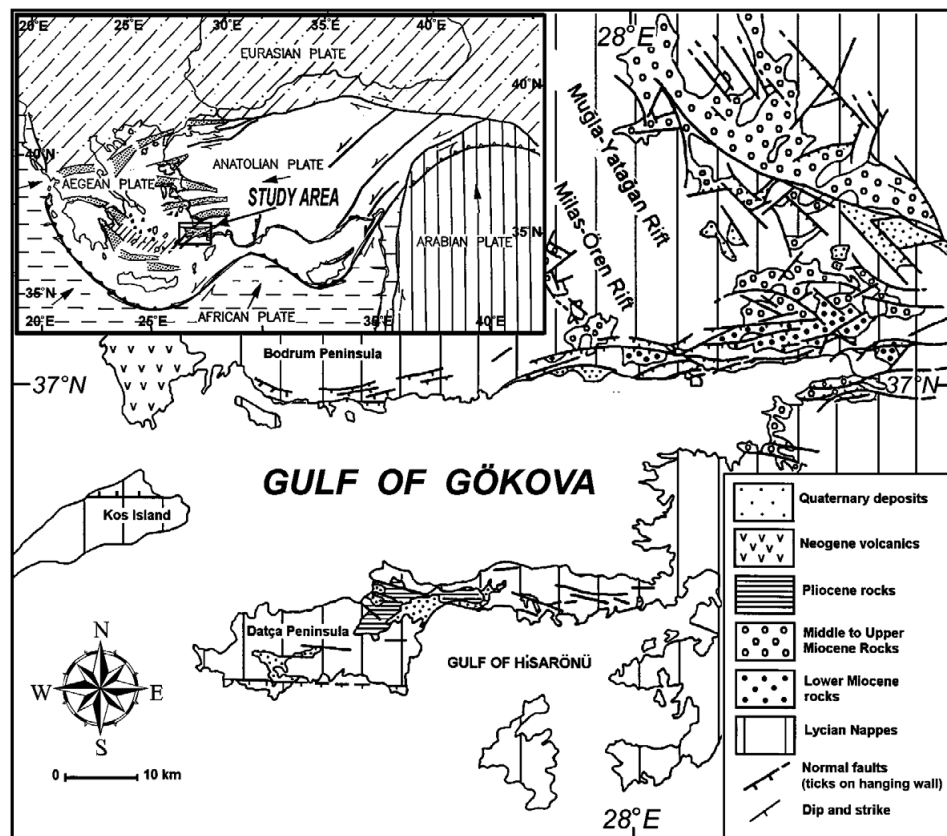
Figure 3.1. Land geology map of the Gökova region (Uluğ *et al*., 2005) (modified from Görür *et al*., 1995). Inset shows the location of the study area and tectonic framework of the Aegean Sea and surrounding regions, compiled from Şengör and Yılmaz (1981), Hancock and Barka (1981) and Dewey *et al*. (1986)

The first studies aiming at investigating the offshore faults were carried out in 1996, and single channel shallow seismic studies were applied especially on the young delta sediments at the eastern part of the gulf (Aktar *et al*., 2006). Studies by Kurt *et al* (1999) gave crucial information about the locations of the faults by utilizing multi channel seismic reflection method (Aktar *et al*., 2006). The result of that study indicated the presence of a major E-W trending north dipping Datça Fault at the southern part of the gulf. They also confirmed the existence of faults to the north but interpreted them as being antithetic with respect to the major southern one (Aktar *et al*., 2006). Besides it was mentioned that the faults located inside the gulf were mainly E-W trending, and there was uncertainty between the eastern and western part of Ören (Aktar *et al*., 2006).

Despite major differences between various authors for the interpretation of the faults trends in Gökova Bay, it remains clear that the main structure is a graben system developing under the influence of the Aegean extensional regime. The area was very active seismically both in historical and instrumental periods. In recent years the area is well observed by a relatively dense network of permanent and temporary stations. In most previous studies, the estimation of the magnitude from the first few seconds of the P-wave was carried out in strike-slip regime. The particular tectonics of the Gökova Gulf provides a first opportunity to test the estimation process in a normal fault environment.

4. SEISMICITY OF GÖKOVA REGION

The Gulf of Gökova is one of the most seismically active places of southwest Anatolia. The region has great importance in terms of having both touristic and industrial areas. It is known that throughout history the region was affected by large-destructive earthquakes. In order to mitigate loss of lives and economic losses from earthquakes, firstly the special features of the active fault zones in the region should be determined by examining the earthquakes occurred from historical times to the present day. For this purpose, it is considerable to study the source parameters of the past events. It is known that many researchers have developed different earthquake catalogues (Tan *et al.*, 2008). Here I made a compilation of all destructive historical events from B.C 412 and the recent ones with magnitudes larger than four.

The first known earthquake in the region occurred in 412 B.C, offshore of the Island of Kos (Soysal *et al.*, 1981). In 141 A.D two large earthquakes were observed around the region (Aktar *et al.*, 2006).

On 18th of August 1493 (Soysal *et al.*, 1981) and 18 October 1493 with Me 6.5 (Guidoboni and Comastri, 2005) two earthquakes occurred around Bodrum which destroyed the city completely.

In 1571, it was mentioned that an earthquake happened at Island of Kos (Ambraseys and Finkel, 1995).

In 1616, an earthquake which devastated almost every house occurred at Rhodes Island (Ambraseys and Finkel, 1995).

In 1631, it was mentioned that a destructive earthquake occurred near Milas (Ambraseys and Finkel, 1995).

In October 1660, a weak earthquake shock was felt at Rhodes Island (Ambraseys and Finkel, 1995).

In March 1673, an earthquake with unknown intensity occurred at the Island of Kos where the chronicles mentioned that 'Stanchio Island with all citizens was absorbed by the sea' (Ambraseys and Finkel, 1995).

In 1685-1686, there are records that a large earthquake occurred which damaged Rhodes Castle (Ambraseys and Finkel, 1995).

In 1714, an earthquake occurred in Island Rhodes which caused cracks in a tower on the island (Ambraseys and Finkel, 1995). It was mentioned that this event was probably the same event which occurred in İzmir in 1713 (Ambraseys and Finkel, 1995).

In 1741, a destructive earthquake occurred at the offshore of Rhodes Island which caused damage in every village and downtown in Rhodes (Ambraseys and Finkel, 1995). It was mentioned that most of the buildings collapsed and the city walls of Rhodes were damaged (Ambraseys and Finkel, 1995).

In 1776, an intense earthquake occurred at Rhodes Island which lasted two minutes (Ambraseys and Finkel, 1995). The earthquake didn't cause much damage in town but large cracks were observed on the ground in rural areas (Ambraseys and Finkel, 1995).

On 26th of June 1926, Kos-Rhodes earthquake occurred with magnitude 7.5 (Uluğ *et al*., 2005).

On 24th of April 1933, an earthquake with magnitude 6.4 occurred at Island of Kos direction (Aktar *et al*., 2006).

On 23th of May 1941, an earthquake with magnitude 6.0 occurred around the vicinity of Ula – Ören (Aktar *et al*., 2006). On 13th of December, Muğla-Bodrum earthquake occurred with magnitude 6.5 (Uluğ *et al*., 2005).

In 1948, Rhodes earthquake occurred with magnitude 7.1 (Uluğ *et al*., 2005).

In 1956, Kos earthquake occurred with magnitude 7.2 (Uluğ *et al*., 2005).

In 1957, Fethiye earthquake occurred with magnitude 7.1 (Uluğ *et al*., 2005).

On 23th of May 1961, an earthquake occurred in Marmaris with magnitude 6.5 (Uluğ *et al*., 2005).

On 1987, around the Island of Rhodes and Marmaris, the earthquake activity began on 1st of January and continued for long time (Kalafat *et al*., 2004). During one month ten earthquakes occurred with magnitudes between 4.0 - 4.4 (Kalafat *et al*., 2004). Especially, two earthquakes which occurred on 4th of April with magnitude 4.6 and on 19th of June with magnitude 5.0, felt around Marmaris-Köyceğiz (Kalafat *et al*., 2004). The earthquake activity continued till the end of the year at Datça-Rhodes-Marmaris region and a total of 25 earthquakes with magnitudes range from 4.0 to 5.1 occurred (Kalafat *et al*., 2004). At the same year 7th of May an event with body wave magnitude, Mb, 4.7 was recorded around Dodecanese Islands (Kalafat *et al*., 2004).

On 27th of April 1989, an earthquake with magnitude 5.3 occurred in the Gulf of Gökova and four earthquakes with magnitudes range from 4.0 to 5.1 occurred during the following two days (Kalafat *et al*., 2004).

In 1990, 21 earthquakes with magnitudes range from 4.0 to 4.8 were observed around Datça-Rhodes-Marmaris in January and the earthquake activity lasted until the middle of May (Kalafat *et al*., 2004). On 25th of May, seismic activity began in Köyceğiz (Kalafat *et al*., 2004). On 28th of August, an event with Mb = 4.6 was felt at Rhodes, Fethiye, Köyceğiz and Marmaris (Kalafat *et al*., 2004).

In 1993, 29th of June an event with Mb = 4.9 was felt around the Island of Karpathos, Rhodes and Dodecanese (Kalafat *et al*., 2004). On 26th of August an earthquake with Mb =5.3, occurred in Marmaris and that event was felt at Rhodes, Marmaris, Kuşadası and Sömbeki, also caused panic due to aftershocks (Kalafat *et al*., 2004). On 9th of January East

Mediterranean earthquake with Mb 4.6 occurred and was felt around Kaş, the Island of Meis, Rhodes and other islands at the vicinity (Kalafat *et al*., 2004). At the same time of the year, seismic activity was also observed around Manavgat, Bodrum, Datça and surrounding regions (Kalafat *et al*., 2004).

In 1996, two earthquakes were observed on 12th of April in Datça with 5.4 and Rhodes with 5.2 (Kalafat *et al*., 2004). On 20th July, an event with magnitude 5.6 occurred around Dodecanese Islands and till the end of September 35 earthquakes with magnitudes 4.0-4.8 were recorded (Kalafat *et al*., 2004). In April the earthquake activity began around Bodrum and 20 earthquakes were recorded in two days (Kalafat *et al*., 2004).

On 5th of October 1999, an earthquake with magnitude 5.6 occurred in Marmaris, and seismic activity in the region was last until the end of the year (Kalafat *et al*., 2004). Between 30th of April and May, 33 events were observed around Muğla-Milas region (Kalafat *et al*., 2004).

In 2004, an earthquake sequence began in the Gulf of Gökova offshore near Çiftlikköy, in Bodrum region (Kalafat *et al*., 2004). On 3rd of August an earthquake with Ml = 5.0 occurred (Kalafat *et al*., 2004). On 4th of August two earthquakes occurred with local magnitudes 5.4 and 5.0 (Kalafat *et al*., 2004). The same day an earthquake was triggered in Milas with Ml 5.0 (Kalafat *et al*., 2004). On 7th of October, an earthquake occurred in Dodecanese Islands with Mb 5.7 (Kalafat *et al*., 2004). Figure 4.1 shows the earthquake activity in the Gulf of Gökova region in the last century and two main shocks occurred on 4th of August 2004 (Kalafat *et al*., 2004).

In 2005, two earthquakes occurred in Bodrum on 10th of January and 11th of January with Ml 5.3 and 5.0, respectively (Kalafat *et al*., 2004).
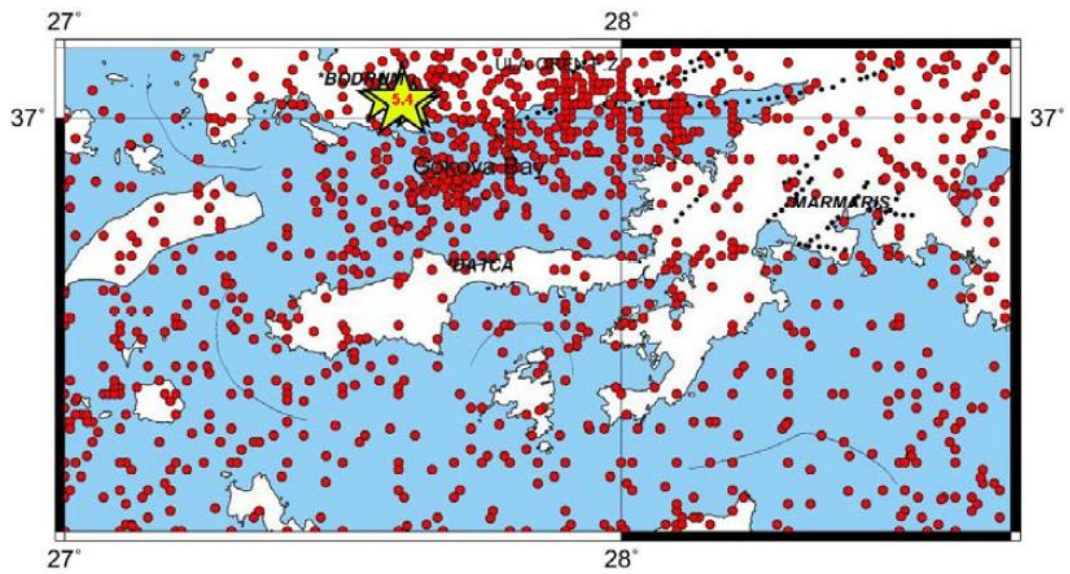
Figure 4.1. Earthquake activity in the Gulf of Gökova region in the last century (Kalafat *et al*., 2004)
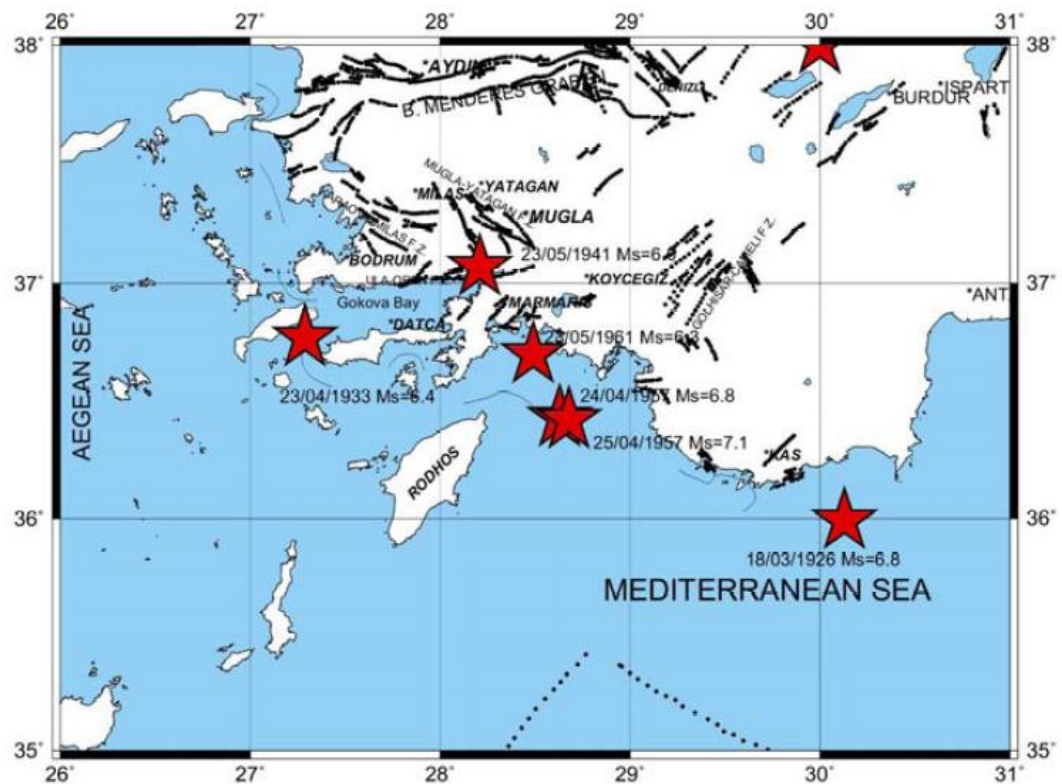

Figure 4.2. The destructive earthquakes of the last century in the Gulf of Gökova region (Kalafat *et al*., 2004)

It is clear that the SW Turkey was seismically very active during both historical and instrumental times. Figure 4.2 shows the destructive earthquakes of the last century around the study region (Kalafat *et al*., 2004). Part of this activity is due to the Eagean Subducting Plate that creates a deep seismic zone connecting Rodos and Fethiye. These events are generally located between 50 and 70 km depth and are not related to the graben structure of the Gökova Bay. Some of the historical earthquakes probably reflect this mechanism. Another part of the historical records probably relates to the western extension of the normal faults that are located in the Gökova Bay. In particular records indicating damages on the island of Kos are likely to occur on the western extension of the faults in Gökova Bay. However it is clear that many of the mentioned events as well as those recorded instrumentally relates directly to the seismic activity in the Gökova Bay.

In recent years the area is well observed by a relatively dense network of permanent and temporary stations. During the last decade, many samples of both medium size events as well as intense swarm activities were efficiently recorded by broadband instruments in the near field. Large number of high quality digital recordings is available for events covering a wide range of magnitudes. This therefore provides a suitable site for the investigation of P-wave magnitude estimation studies. Considering also the fact that the area experiences a rapidly growing population in cities like Bodrum, Marmaris, and Milas, the results obtained would also be useful for the implementation of a future Early Warning System in the Gulf of Gökova. One must also emphasize that a large earthquake in the gulf will not only cause damage to structures trough ground shaking but would also create a serious hazard trough tsunami generation as it has been observed in the past.

5. DATA

Two data sets were used in this study. The former one was obtained from one month continuous signal that were recorded by NEMC's seven permanent broadband stations called BLCB, BODT, DALT, DAT, ELL, MLSB, YER located around Gökova region (Figure 5.1). Apart from these broadband stations, three temporary stations were also used (called OZCA, CETI and TURG) which were installed in 2005 within the framework of a project supported by TUBITAK (Figure 5.1) (Aktar *et al.*, 2006). Figure 5.3 shows the site for the station BODT which, although located next to high antennas, still gives a high SNR because its location on hard rock and its sensor buried in a deep hole. Figure 5.4 shows the installation of the temporary station on TURG. This station also gives a high SNR signal due to its location on hard rock with cement basement and also due to its relatively high distance to the nearest noise source (a house in this case) being more than 200 m. Although all 10 stations mentioned above were in full operation during the month of August 2007, not all of them were always used to locate the events. DAT station had GPS problem, therefore it was only used to calculate the local magnitudes of the events (Figure 5.2). Horizontal components were not in operation in OZCA which made it difficult to read S-phases and CETI station had a lower SNR due to its location closer to a highway. Nevertheless it was possible to make a very fine analysis of the seismicity for the time period that was analysed. The improvement in the detection level as compared to the routine location processes carried out in NEMC was considerable and will be shown below.

The second data set that I used was directly taken from the NEMC catalogue because it covers larger time scale (from 2006 to 2010). This second catalogue which only includes large events between magnitudes ranges from 3.5 to 5.1. It consists of 30 earthquakes occurred around Gökova region with local recorded by BLCB, BODT, DALT, DAT, ELL, FETY, MLSB and YER (Table 6.1).
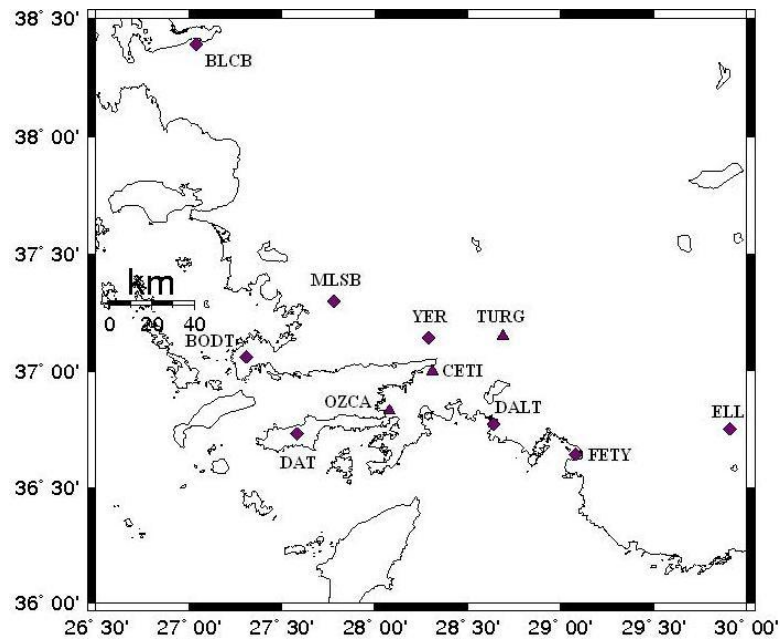
Figure 5.1. The map of the stations that are used in this study. Purple diamonds indicate permanent, triangles indicate temporary broadband stations
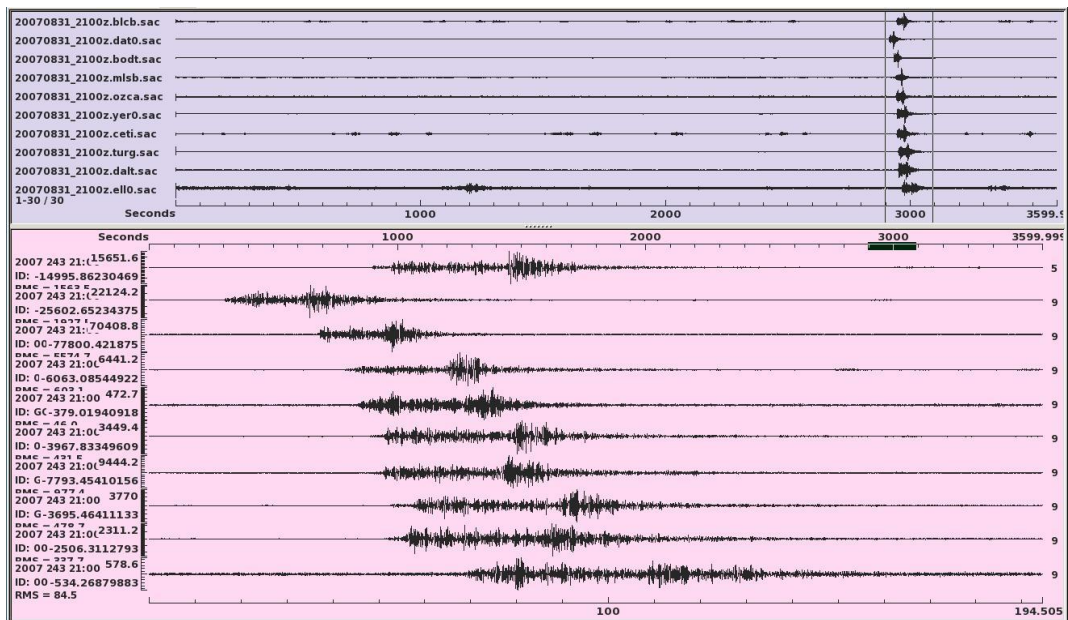
Figure 5.2. The figure showing the GPS problem at DAT station. The seismic traces in the figure belong to an earthquake occurring at Lat. 36.922N and Lon. 27.395E, hence BODT station should record this event first but because of the GPS problem, DAT station seems to record first

Figure 5.3. The site for the permanent BODT station near Bodrum (from NEMC Report , 14 February 2005)

Figure 5.4. Installation of the seismometer at the station TURG on 15 December 2006

The permanent stations around the gulf (BODT, DALT, DAT, ELL, FETY, MLSB, YER) were installed by NEMC. By the beginning of 2004 the older seismometers were replaced with the newer ones. All the permanent broadband stations were installed with CMG-3T ESP type of seismometer with frequency band 0.012-25 Hz and GPS system were used for time synchronization (Aktar *et al*., 2006).

The temporary stations (OZCA, CETI, TURG) were installed with GURALP CMG-6T type of seismometer with frequency band 0.03-25 Hz and GPS system were used for time synchronization (Aktar *et al*., 2006).

5.1. Data Preparation

The recordings were monitored in PQLII (PASSCAL Quick Look) (PASSCAL, 2008) seismic trace viewer application. The filtering and phase picking were carried out by this program. Bandpass filter with cutoff frequencies between 2.0 Hz -12 Hz were applied to filter the data. After filtering and P, S phase picking, the pick files were converted to Nordic format in order to locate events by HYPO program (The hypocenter program) (Havskov and Ottemöller, 2005). The local magnitudes of the earthquakes were calculated using the following relation (Havskov and Ottemöller, 2005);

$$Ml = log\ (amp) + 1.11\ log\ (dist) + 0.00189\ dist - 2.09 \tag{5.1}$$

We prefer to calculate local magnitudes with this equation because it is more labor saving than the others. We also did not applied a routine to remove the instrument response by pole-zero correction since the response of the broadband sensors is fairly flat in the frequency band covered by the standard Wood-Anderson seismometer. The final effect of this approximation is not expected to be more than 0.1 magnitude in the final analysis.

After processing one month recordings at 10 stations, a total of 985 events were detected and the locations of the events were plotted using EPİMAP tool of SEISAN program (Havskov and Ottemöller, 2005). The Figure 5.5 shows the locations of 973 events, the ones excluded include only the regional or the teleseismic events.
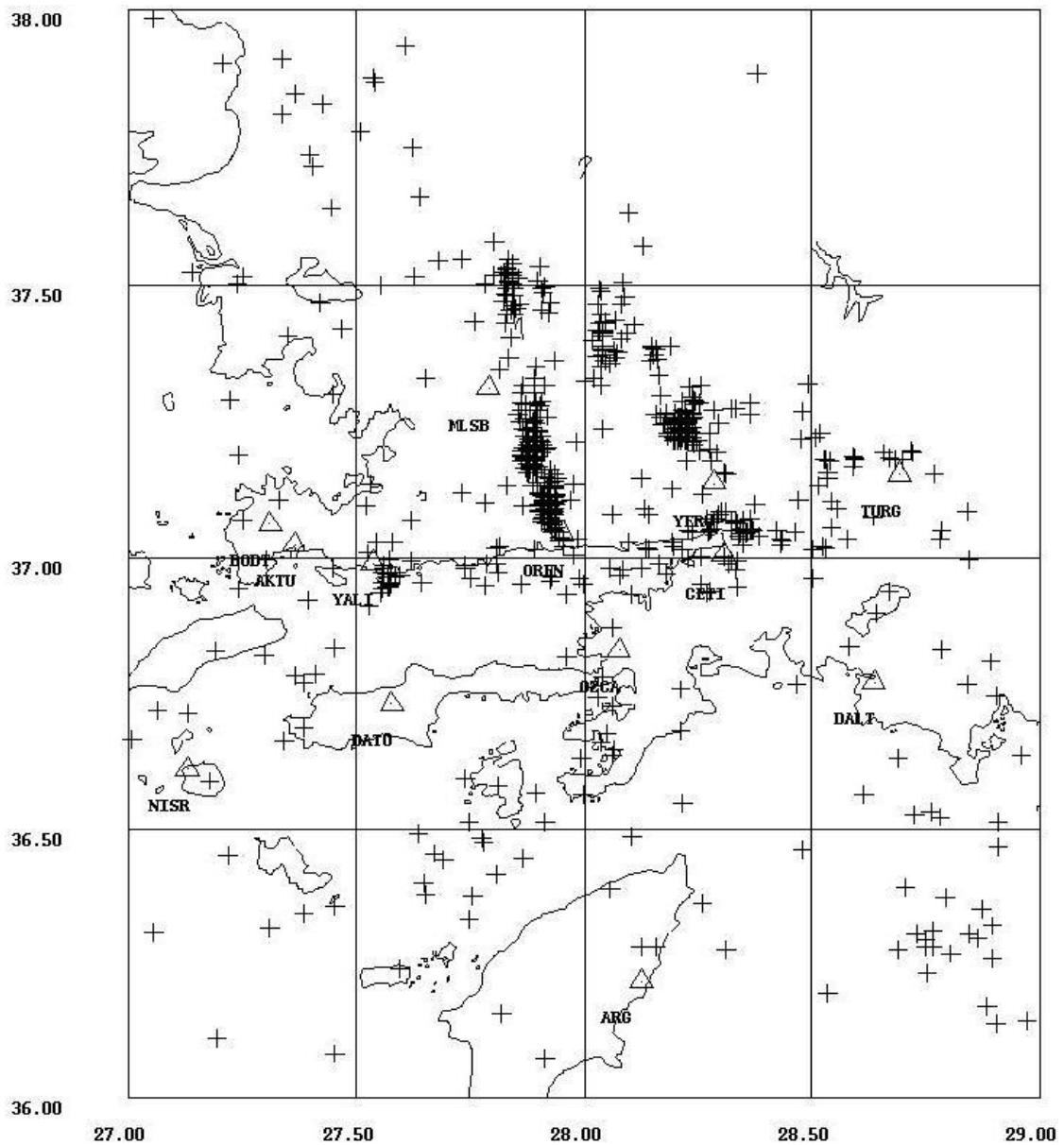
Figure 5.5. The location of events occurred in August 2007

5.2. Data Analysis

I compare our one month events that I found with August 2007 catalogue of NEMC in four ways. Firstly, in order to form a general judgment I plotted events according to their depths. Secondly, I plotted events according to their magnitudes. Thirdly, I draw a histogram to compare the magnitudes and number of earthquakes, and finally I calculated b-values of the data sets to examine the lowest magnitude that are detected with confidence in both catalogues, in other word their completeness thresholds.
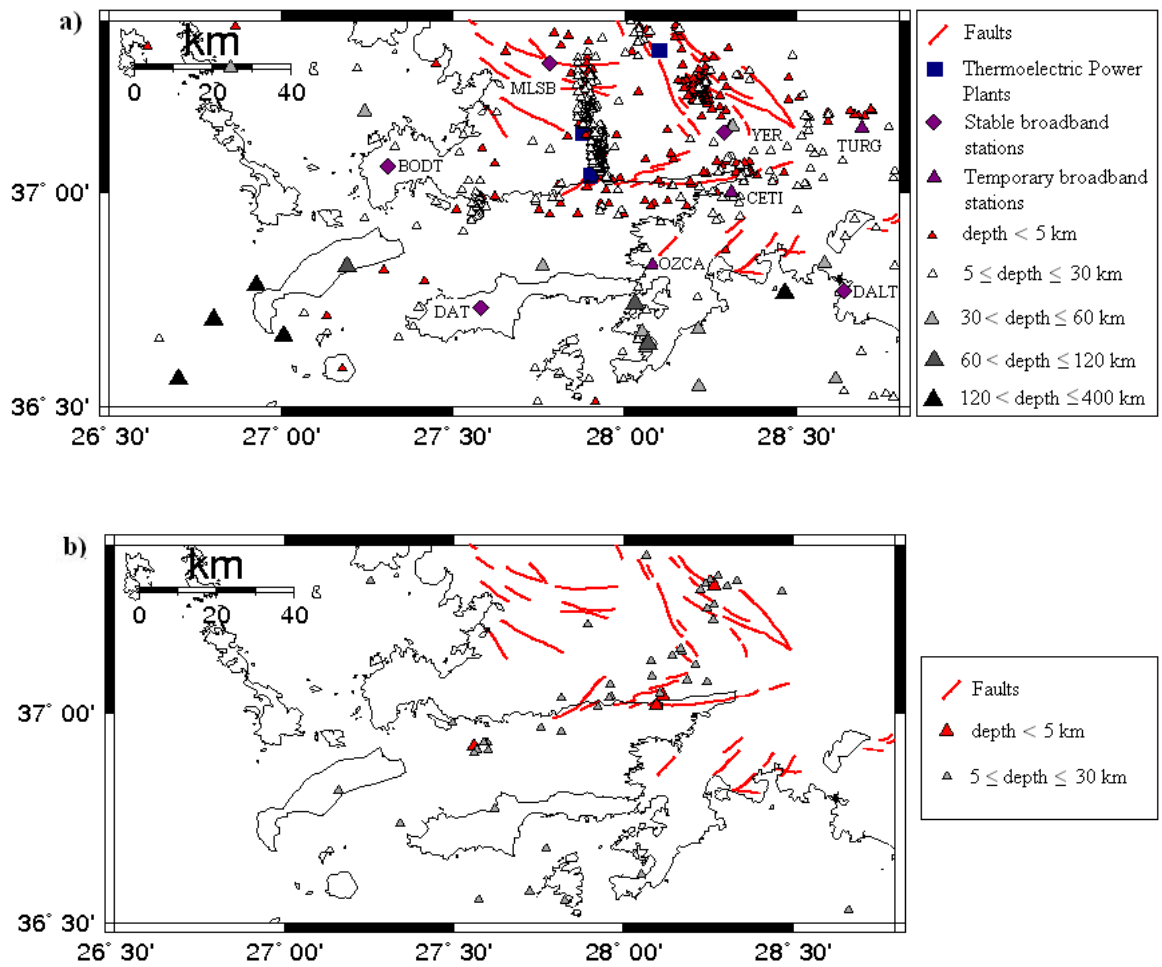
Figure 5.6. The location of events occurred in August 2007, according to their depths.

a) Thesis result b) NEMC catalogue
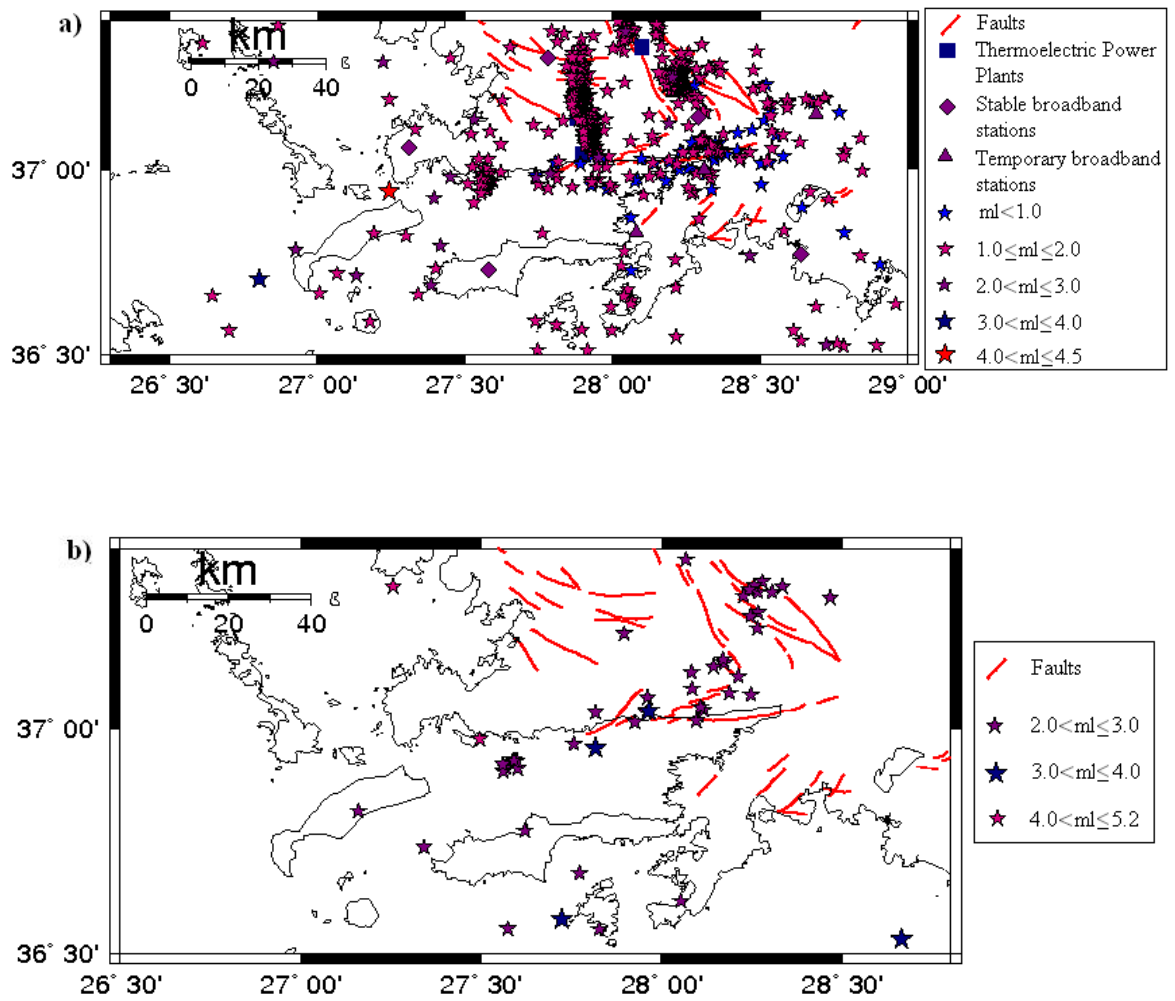
Figure 5.7. The location of events occurred in August 2007, according to their local magnitudes. a) Thesis result. b) NEMC catalogue
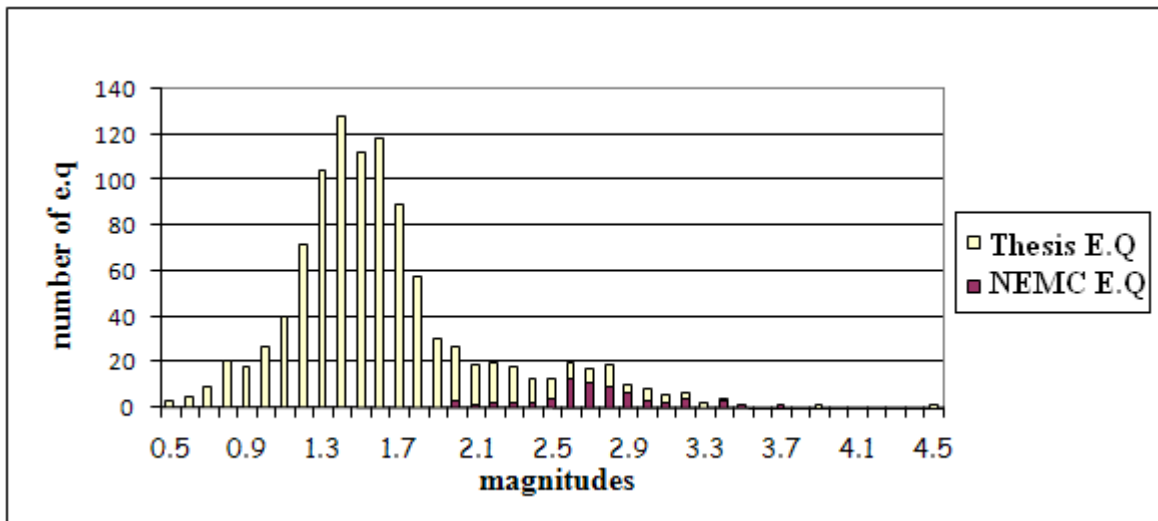
Figure 5.8. The histogram of the number of earthquake with respect to their magnitude
(solid columns: NEMC catalogue, empty columns: this thesis)

In probabilistic hazard assessments, seismicity data have been generally used for projecting future events (Yeats *et al*., 1997). According to Gutenberg and Richter (1954) earthquake magnitude and frequency have a systematic relationship with each other (Yeats *et al*., 1997). The relationship was expressed in Gutenberg-Richter recurrence relationship as (Yeats *et al*., 1997),

$$Log\ N = a - bM \tag{5.2}$$

The values of a and b are found by using least squares estimation,

$$a = [\sum_{i=1}^{n} M_i{}^2 \sum_{i=1}^{n} \log N_i - \sum_{i=1}^{n} M_i \sum_{i=1}^{n} M_i \log N_i][\ n\sum_{i=1}^{n} M_i{}^2 - (\sum_{i=1}^{n} M_i)^2]^{-1} \tag{5.3}$$

$$b = [\sum_{i=1}^{n} M_i \sum_{i=1}^{n} \log N_i - n\sum_{i=1}^{n} M_i \log N_i][\ n\sum_{i=1}^{n} M_i{}^2 - (\sum_{i=1}^{n} M_i)^2\ ]^{-1} \tag{5.4}$$

Table 5.1. Earthquake data used in our study in order to find *b* value

i	Magnitude	Number of E.Q	N(M)	Log N(M)	M*Log N(M)	M**2
1	1.4	128	674	2.828659897	3.960123855	01.96
2	1.5	112	546	2.737192643	4.105788964	02.25
3	1.6	118	434	2.63748973	4.219983567	02.56
4	1.7	89	316	2.499687083	4.24946804	02.89
5	1.8	58	227	2.356025857	4.240846543	03.24
6	1.9	30	169	2.227886705	4.232984739	03.61
7	2.0	24	139	2.1430148	4.286029601	04.00
8	2.1	18	115	2.06069784	4.327465465	04.41
9	2.2	18	97	1.986771734	4.370897815	04.84
10	2.3	16	79	1.897627091	4.36454231	05.29
11	2.4	11	63	1.799340549	4.318417319	05.76
12	2.5	9	52	1.716003344	4.290008359	06.25
13	2.6	7	43	1.633468456	4.247017985	06.76
14	2.7	6	36	1.556302501	4.202016752	07.29
15	2.8	10	30	1.477121255	4.135939513	07.84
16	2.9	3	20	1.301029996	3.772986987	08.41
17	3.0	5	17	1.230448921	3.691346764	09.00
18	3.1	4	12	1.079181246	3.345461863	09.61
19	3.2	3	8	0.903089987	2.889887958	10.24
20	3.3	2	5	0.698970004	2.306601014	10.89
21	3.4	1	3	0.477121255	1.622212266	11.56
22	3.5	0	2	0.301029996	1.053604985	12.25
23	3.6	0	2	0.301029996	1.083707984	12.96
24	3.7	0	2	0.301029996	1.113810984	13.69
25	3.8	0	2	0.301029996	1.143913984	14.44
26	3.9	1	2	0.301029996	1.174016983	15.21
27	4.0	0	1	0	0	16.00
28	4.1	0	1	0	0	16.81
29	4.2	0	1	0	0	17.64
30	4.3	0	1	0	0	18.49
31	4.4	0	1	0	0	19.36
32	4.5	1	1	0	0	20.25
Total	94.4	674	3101	38.75228087	86.7490826	305.76
Aver	2.95			1.211008777		
i	32					
a=	1.770366978					
b=	1.010635849					
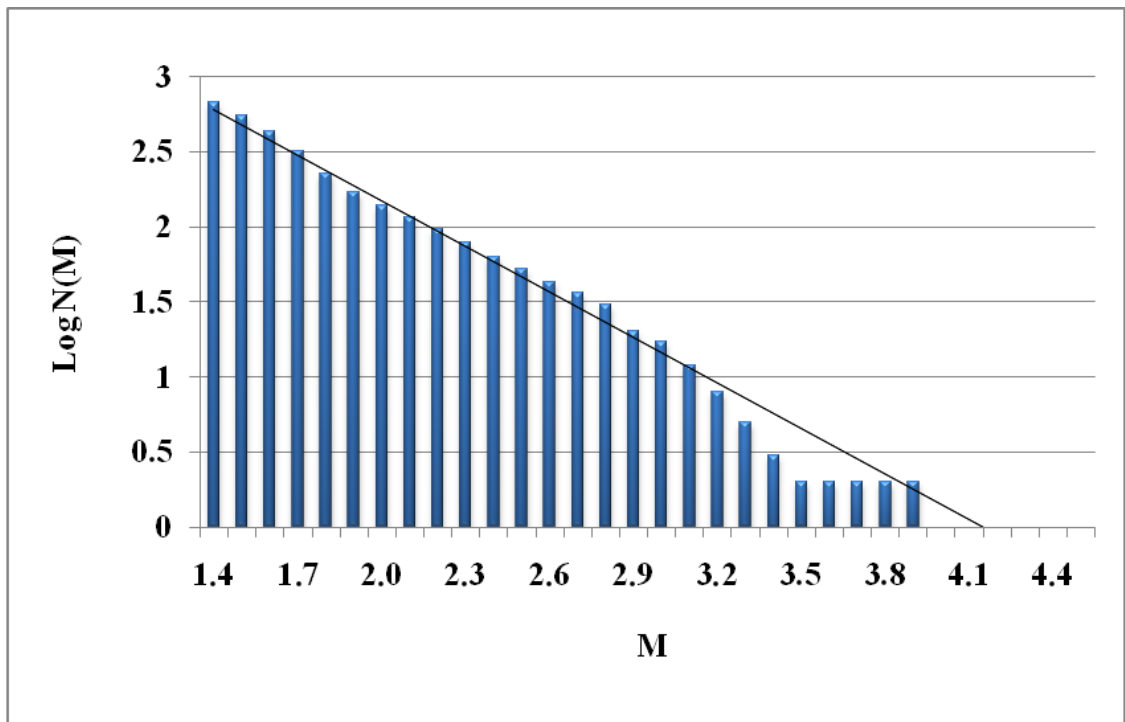
Figure 5.9. The histogram of the logarithm of the number of events versus their magnitudes
(Our result)

Figure 5.9 is the recurrence curve of our data with 0.1 intervals. The straight-line fit is made by least-squares. Table 5.1 shows the calculation steps that I prepared in Microsoft Excel program. The completeness value, Mc, is observed as 1.4 and the b value of our data set is calculated as 1.01.

Table 5.2. Earthquake data used in NEMC's catalogue in order to find b value

i	Magnitude	Number of E.Q	N(M)	Log N(M)	M*Log N(M)	M**2
1	2.6	13	54	1.73239376	4.504223776	06.76
2	2.7	11	41	1.612783857	4.354516413	07.29
3	2.8	9	30	1.477121255	4.135939513	07.84
4	2.9	7	21	1.322219295	3.834435955	08.41
5	3.0	3	14	1.146128036	3.438384107	09.00
6	3.1	2	11	1.041392685	3.228317324	09.61
7	3.2	4	9	0.954242509	3.05357603	10.24
8	3.3	0	5	0.698970004	2.306601014	10.89
9	3.4	3	5	0.698970004	2.376498015	11.56
10	3.5	1	2	0.301029996	1.053604985	12.25
11	3.6	0	1	0	0	12.96
12	3.7	1	1	0	0	13.69
Total	37.8	54	194	10.9852514	32.28609713	120.5
Aver	3.15			0.915437617		
i	12					
a=	4.189423263					
b=	1.620590755					
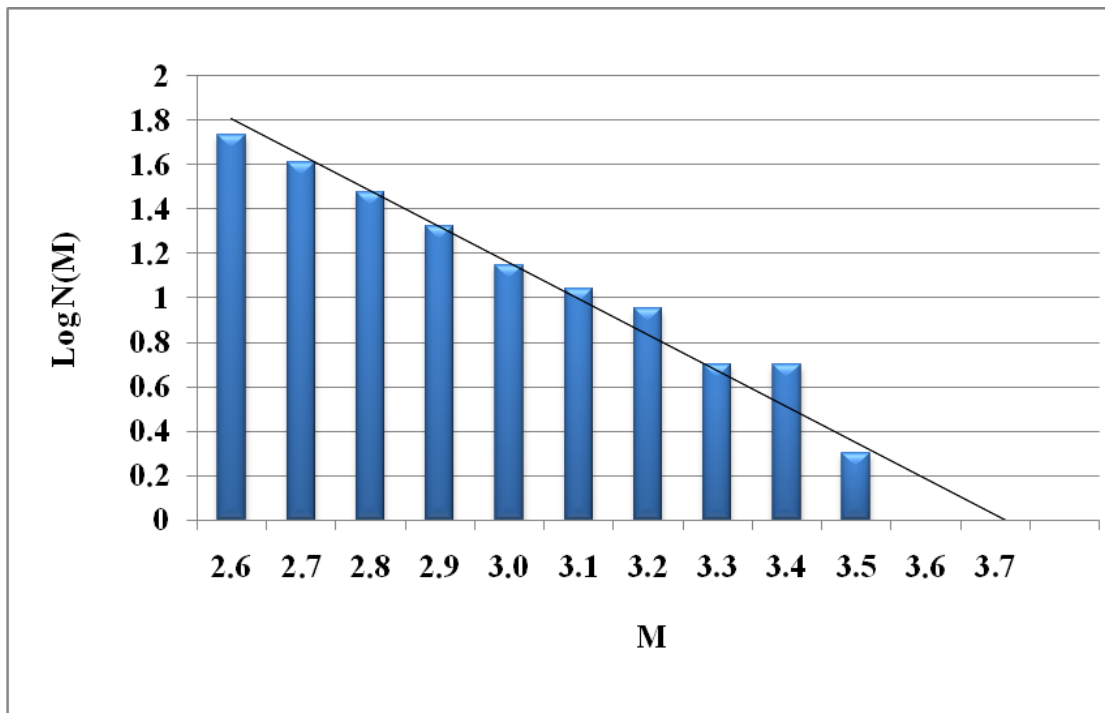
Figure 5.10. The histogram of the logarithm of the number of earthquakes versus their
magnitudes (NEMC catalogue)

Figure 5.10 is the recurrence curve of NEMC's data with 0.1 intervals. The straight-line fit is made by least-squares. The Mc value is observed as 2.6, at the end of Table 5.2, b value is given as 1.62. Although the two catalogues (NEMC and this thesis) cover the same period of time (August 2007) b values are very differing from each other.

As we can see from the figures, there is a large difference between the two data sets in terms of detection capability. In accordance with our results, we detected 973 events, while the number of events that were taken from NEMC catalogue were 68. According to my point of view this dramatic difference is due to two reasons. Our data set include explosions that are generated by three thermoelectric power plants which are located around Yatağan, and mines around Gökova region which are of magnitude less than 2.0. On the other side, NEMC catalogue does not include events Ml < = 2.0 which therefore exclude many of the explosions. On account of abolishing the variation between the data sets, I differentiate explosions from earthquakes and eliminate them from the catalogue and I repeat all the process as mentioned above.

In order to distinguish explosions from earthquakes, I draw a histogram showing the number of earthquakes and their occurrence times. I choose two dense regions to see the time dispersion of events.
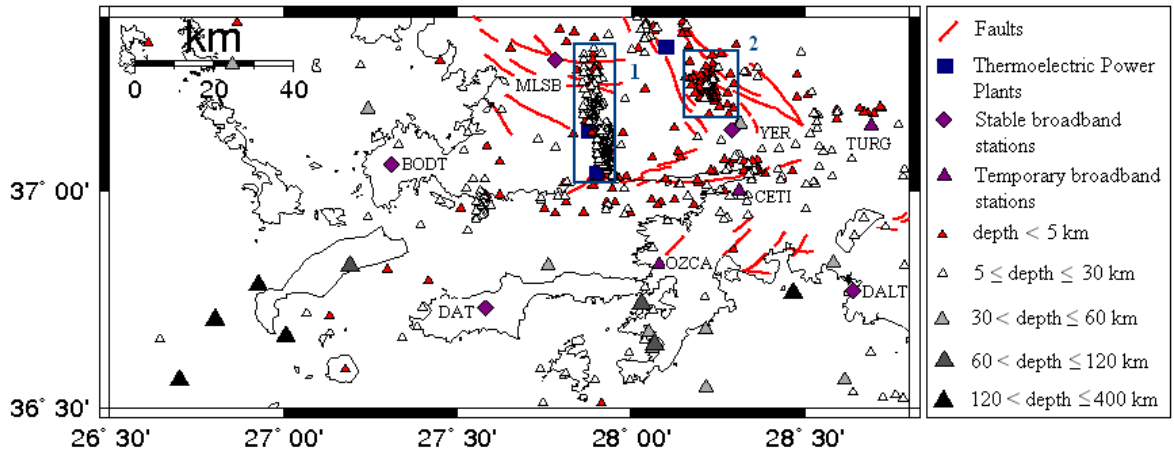
Figure 5.11. The map showing the selected two dense regions. The first frame indicates events with Latitude: 36.99 – 37.30 Longitude: 27.62 – 28.00, the second frame Latitude: 37.20 – 37.30 Longitude: 28.05 – 28.30

Table 5.3. The time dispersion of events in the first frame

Time	Number of E.Q
00:00	1
01:00	3
02:00	3
03:00	3
04:00	1
05:00	5
06:00	9
07:00	23
08:00	56
09:00	45
10:00	8
11:00	16
12:00	19

13:00	26
14:00	59
15:00	12
16:00	0
17:00	0
18:00	1
19:00	0
20:00	1
21:00	0
22:00	0
23:00	0
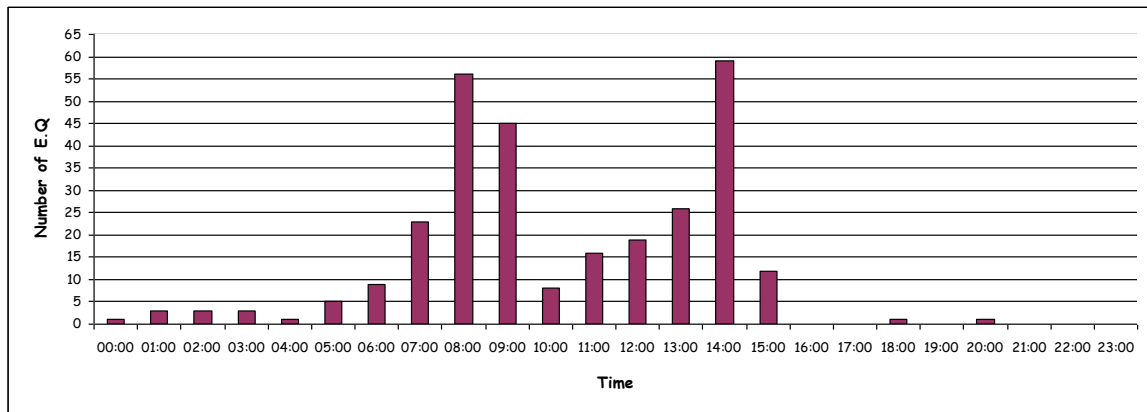
Figure 5.12. The histogram of the number of earthquakes and their occurrence times
(Frame1)

Table 5.4. The time dispersion of events in the second frame

Time	Number of E.Q
00:00	0
01:00	0
02:00	0
03:00	0
04:00	0
05:00	5
06:00	6
07:00	8
08:00	3
09:00	48
10:00	1
11:00	1
12:00	4
13:00	3
14:00	1
15:00	66
16:00	0
17:00	0
18:00	0
19:00	0
20:00	0
21:00	0
22:00	0
23:00	0
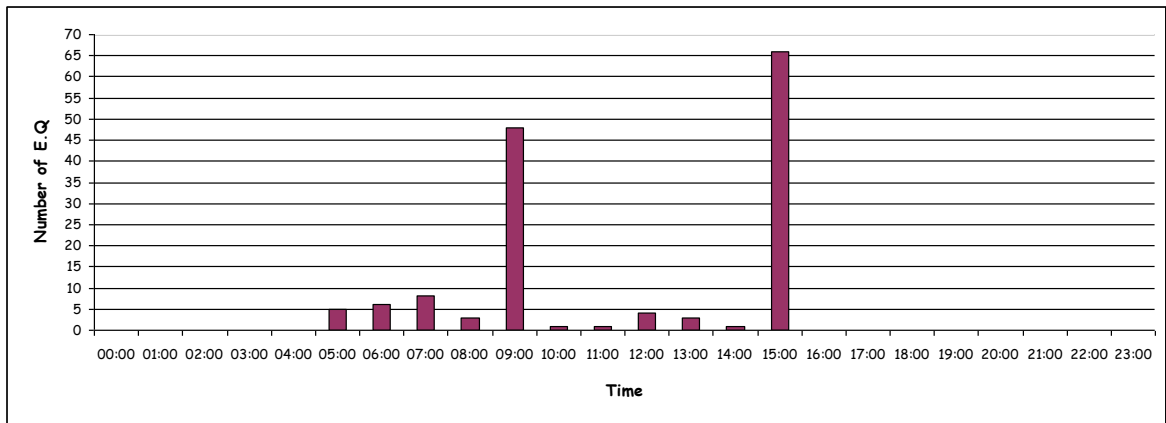
Figure 5.13. The histogram of the number of earthquakes and their occurrence times (Frame2)

Figure 5.12 shows us that between 06:00 am and 15:00 pm the number of events increases dramatically. The increases of events are more evident in Figure 5.13. If we take into account that the region is so active in terms of mining activities, it will not be wrong to think that explosions might be the explanation of this increase. Consequently, I eliminated events in Frame-1 which occurred between 06:00 am and 15:00 pm, and in Frame-2 between 09:00 am and 15:00 pm, as being explosions. Totally I marked 373 events as explosions within 973 events. After removing the explosions from our data set, I obtain new figures with seismicities having slightly less number of events,
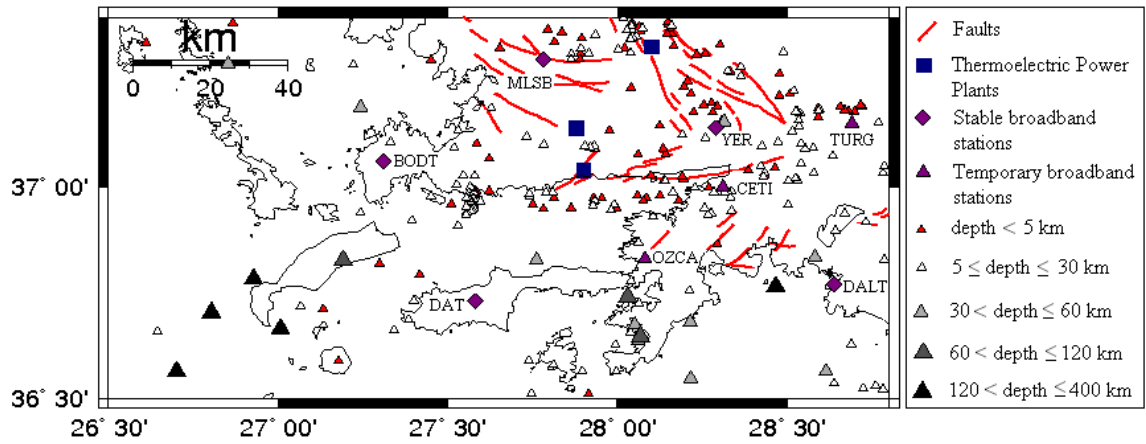
Figure 5.14. The location of earthquakes occurred in August 2007 after removing explosions, according to their depths
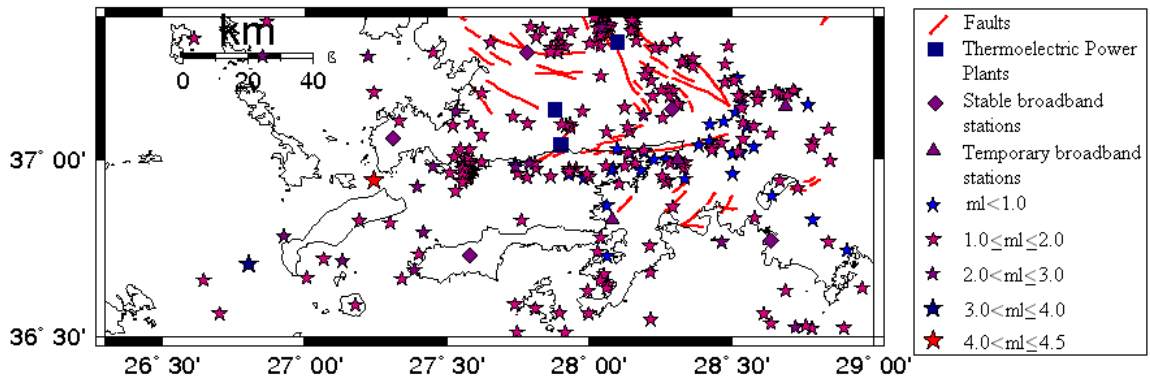
Figure 5.15. The location of events occurred in August 2007 after removing explosions, according to their local magnitudes
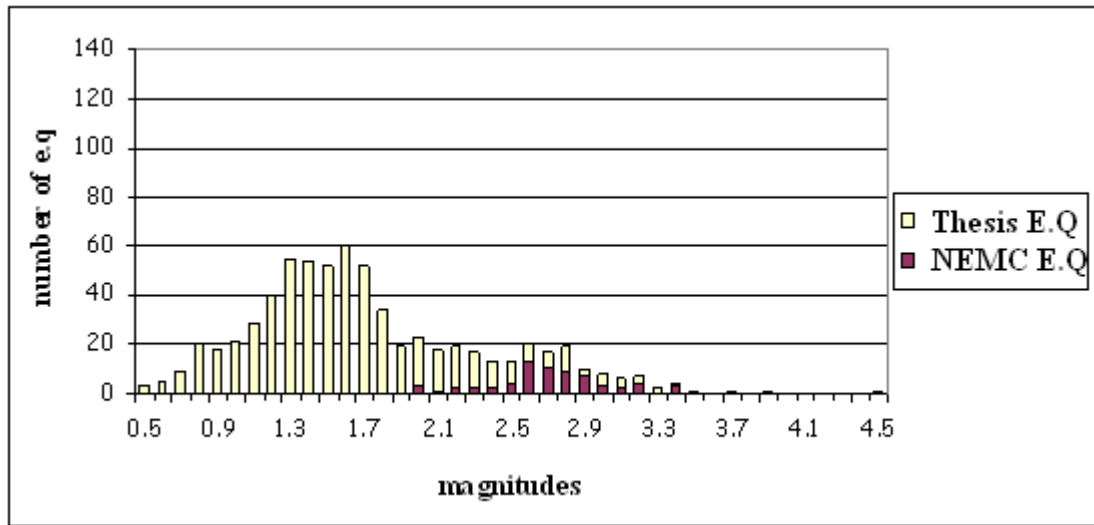
Figure 5.16. The histogram of the magnitude and number of earthquake relation between two data sets after removing the explosions

Table 5.5. Earthquake data used in our study in order to find b value after removing the explosions

i	Magnitude	Number of E.Q	N(M)	Log N(M)	M*Log N(M)	M**2
1	1.4	54	404	2.606381365	3.648933911	01.96
2	1.5	51	350	2.544068044	3.816102067	02.25
3	1.6	61	299	2.475671188	3.961073901	02.56
4	1.7	52	238	2.376576957	4.040180827	02.89
5	1.8	35	186	2.269512944	4.0851233	03.24
6	1.9	19	151	2.178976947	4.1400562	03.61
7	2.0	20	132	2.120573931	4.241147862	04.00
8	2.1	17	112	2.049218023	4.303357848	04.41
9	2.2	17	95	1.977723605	4.350991932	04.84
10	2.3	15	78	1.892094603	4.351817586	05.29
11	2.4	11	63	1.799340549	4.318417319	05.76
12	2.5	9	52	1.716003344	4.290008359	06.25
13	2.6	7	43	1.633468456	4.247017985	06.76
14	2.7	6	36	1.556302501	4.202016752	07.29
15	2.8	10	30	1.477121255	4.135939513	07.84
16	2.9	3	20	1.301029996	3.772986987	08.41

17	3.0	5	17	1.230448921	3.691346764	09.00
18	3.1	4	12	1.079181246	3.345461863	09.61
19	3.2	3	8	0.903089987	2.889887958	10.24
20	3.3	2	5	0.698970004	2.306601014	10.89
21	3.4	1	3	0.477121255	1.622212266	11.56
22	3.5	0	2	0.301029996	1.053604985	12.25
23	3.6	0	2	0.301029996	1.083707984	12.96
24	3.7	0	2	0.301029996	1.113810984	13.69
25	3.8	0	2	0.301029996	1.143913984	14.44
26	3.9	1	2	0.301029996	1.174016983	15.21
27	4.0	0	1	0	0	16.00
28	4.1	0	1	0	0	16.81
29	4.2	0	1	0	0	17.64
30	4.3	0	1	0	0	18.49
31	4.4	0	1	0	0	19.36
32	4.5	1	1	0	0	20.25
Total	94.4	404	2350	37.8680251	85.32973713	305.76
Aver	2.95			1.183375784		
i	32					
a=	1.669401484					
b=	0.967043142					
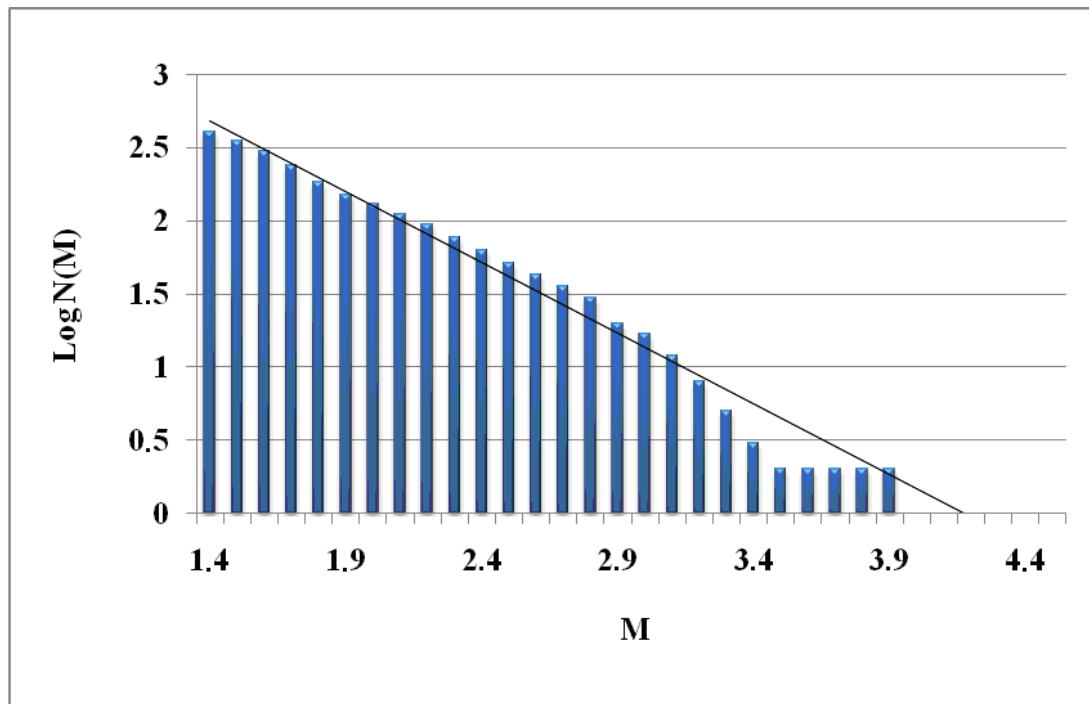
Figure 5.17. The histogram of the logarithm of the number of earthquakes versus their magnitudes after removing the explosions

After removing explosions from our data set, the b-value estimated from our data decreases to 0.97 and this value is more acceptable according to Gutenberg-Richter law, on the other hand, the b-value of the region calculated from NEMC's data set at the same time period was 1.6. According to Gutenberg-Richter law the b-value should be typically equal to 1.0. The overestimation in NEMC's result might depend on three reasons such as using smaller completeness threshold than tactually required for the NEMC catalogue, using data with wrong magnitudes and finally using small data set (Felzer, 2006).

The systematic comparison of the NEMC catalogue with the catalogue produced during the thesis reveals many important points. First of all there is a drastic difference between the two datasets in terms of lower magnitude threshold: Mc=1.4 (this study and Mc>2.6 (NEMC-catalogue). This is normal in a way because the NEMC catalogue does not attempt to make an exhaustive analysis in particular for microseismic events of magnitude less than 2.0. It is important however to take this point into consideration when making any detailed analysis of the local seismicity trough a general catalogue like the one produced by NEMC. As an example one can point that the b-value estimation from the

same period gives two very different values for the catalogues, one being unusually high as to be rejected at the end. Any catalogue at this scale (*i.e.* national scale) would best be used as a starting point for developing more complete ones trough detailed studies. This is exactly the same reason that I reprocessed the August 2007 data in order to base my subsequent studies onto a more complete catalogue.

6. THE ElarmS METHODOLOGY and APPLICATION ACROSS GÖKOVA REGION

The ElarmS methodology was designed to predict the potential distribution of peak ground motion across the risky region affected by an earthquake before the origin of the significant ground motion at the epicenter (Allen, 2007). The first few seconds of the P-wave at the closest stations to the epicenter is used to locate and estimate the magnitude of an earthquake and predict the distribution of ground shaking using the attenuation relations (Allen, 2007). The goal of the ElarmS is to generate a ShakeMap of predicted peak ground shaking which is called AlertMap that can be prepared one sec after the first P-wave arrives to the closest station to the epicenter and can be updated every second as additional data trigger to the stations farther from the epicenter (Allen, 2007). In this study, I describe the first component of the ElarmS and test the availability of determining the magnitude of events from the first few seconds of the P-wave arrivals across Gökova region.

6.1. Datasets

Two datasets were used in this study in order to test the ElarmS system around Gökova region. The first one consists of 600 earthquakes ranging in magnitude from 0.5 to 4.5 that occurred in August 2007 around the study region, and which consists of data entirely processed within the framework of this thesis. There were 468 events with magnitude between 0.5 and 2.0, 120 of them with 2.1 and 3.0, and 12 of them were larger than 3.0. Since I wanted to extend the analysis to larger events and due to the absence of the moderate size earthquakes during this 31 days of study, I included 30 events from outside this time window, with magnitudes ranging from 3.5 to 5.1 and taken from the catalogue of NEMC (Table 6.1). From the catalogue of 2006, I selected six earthquakes ranging in magnitude between 4.1 and 4.6, from 2007 I selected 16 earthquakes with magnitudes between 3.7 and 5.1, from 2008 I selected three earthquakes magnitudes ranging from 3.5 to 3.7, from 2009 I selected four earthquakes magnitudes ranging from 3.5 to 3.7, and finally I selected one earthquake from 2010 with magnitude 3.6. The magnitudes of the earthquakes which were selected from the catalogues were recalculated due to the fact that, NEMC mostly doesn't calculate the local magnitudes of the events.

SAC program was used in order to pick P-phases and a shell script was written for the calculation of the ml magnitudes of the events. Figure 6.1 shows the location of the selected earthquakes according to their local magnitudes.

We could not select events that occurred before 2006 because the number of stations around Gökova region was not sufficient at that time and most of the ones which were in operation used short-period seismometers.

Table 6.1. Event source parameters of the second data set

Date	Time	Magnitude	Latitude	Longitude	Depth	Number of broadband waveforms recorded
20/01/06	09:39:06	4.5	36.97	28.30	11	2
20/01/06	10:40:00	4.5	36.98	28.25	8	2
17/04/06	11:53:00	4.6	37.01	28.31	9	4
17/04/06	19:00:00	4.1	37:03	28.27		2
17/04/06	20:18:00	4.4	37.03	28.25	15	3
18/04/06	01:21:00	4.2	37.01	28.28	3	3
31/01/07	23:13:46	3.9	36.97	27.80	11	8
15/02/07	03:15:53	4.7	36.08	28.00	86	4
22/02/07	16:13:36	4.1	36.71	27.10	131	6
05/03/07	08:24:39	4.7	36.60	26.88	137	7
21/05/07	07:30:52	3.8	36.76	27.62	5	3
11/08/07	01:50:39	4.1	37.05	27.96	14	7
05/09/07	08:19:16	3.7	37.26	27.06	4	6
09/09/07	18:54:39	3.9	36.70	26.91	10	5
23/09/07	17:05:29	4.1	36.92	27.48	3	4
23/09/07	17:09:18	3.9	37.04	27.49	9	4
23/09/07	17:20:59	3.7	36.90	27.49	5	4
10/10/07	21:27:49	3.9	36.63	27.95	94	7
12/10/07	17:06:01	4.2	36.35	27.95	65	3

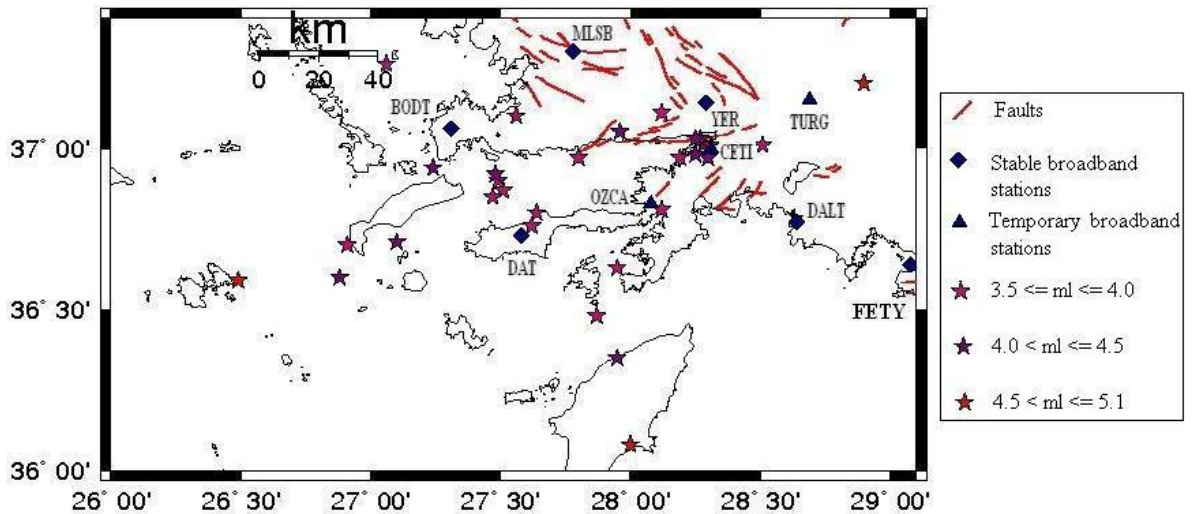| 03/11/07	04:24:23	4.9	36.59	26.49	122	6
25/11/07	05:57:46	5.1	37.20	28.90	4	3
07/12/07	12:57:27	3.9	36.48	27.87	82	7
10/04/08	13:14:56	3.5	37.10	27.56	2	6
03/05/08	15:08:26	3.7	36.87	27.51	7	7
24/09/08	16:16:19	3.6	36.81	28.12	81	6
29/01/09	20:30:20	3.5	36.97	28:19		4
06/02/09	23:51:18	3.7	36.80	27.64		3
01/03/09	03:26:13	3.5	37.11	28.12		3
25/12/09	10:24:46	3.6	36.85	27.47		3
25/02/10	14:50:30	3.6	37.01	28.51		4

Figure 6.1. The location of the second data set according to their magnitudes

6.2. Predominant Period Observations

The rapid estimation of the magnitude of an earthquake is based on measuring the frequency content of the P-wave in first four sec, namely analysing the predominant period of the seismic signal (Allen, 2007). The predominant period, τ_p, is calculated continuously from the vertical component of velocity records using the method first described by Nakamura (1988), and the maximum value, τ_p^{max}, within four sec is calculated in order to scale with event magnitude (Allen and Kanamori, 2003). τ_p is determined using the relation

$$\tau i^{P} = 2\pi\sqrt{Xi/Di} \tag{6.1}$$

where

$$X_i = \alpha X_{i-1} + x_i^{2} \tag{6.2}$$

$$D_i = \alpha D_{i-1} + (dx/dt)_i^{2} \tag{6.3}$$

τ_i^{P} is the predominant period for sample i, x_i is the ground velocity recorded at time i, X_i is the smoothed ground velocity squared at time i, D_i is the smoothed velocity derivatived squared, and α is the smoothing constant for 1.0 sec and equal to 0.99 (Allen and Kanamori, 2003). Figure 6.2 shows an example of this algorithm on a velocity record of BODT station.
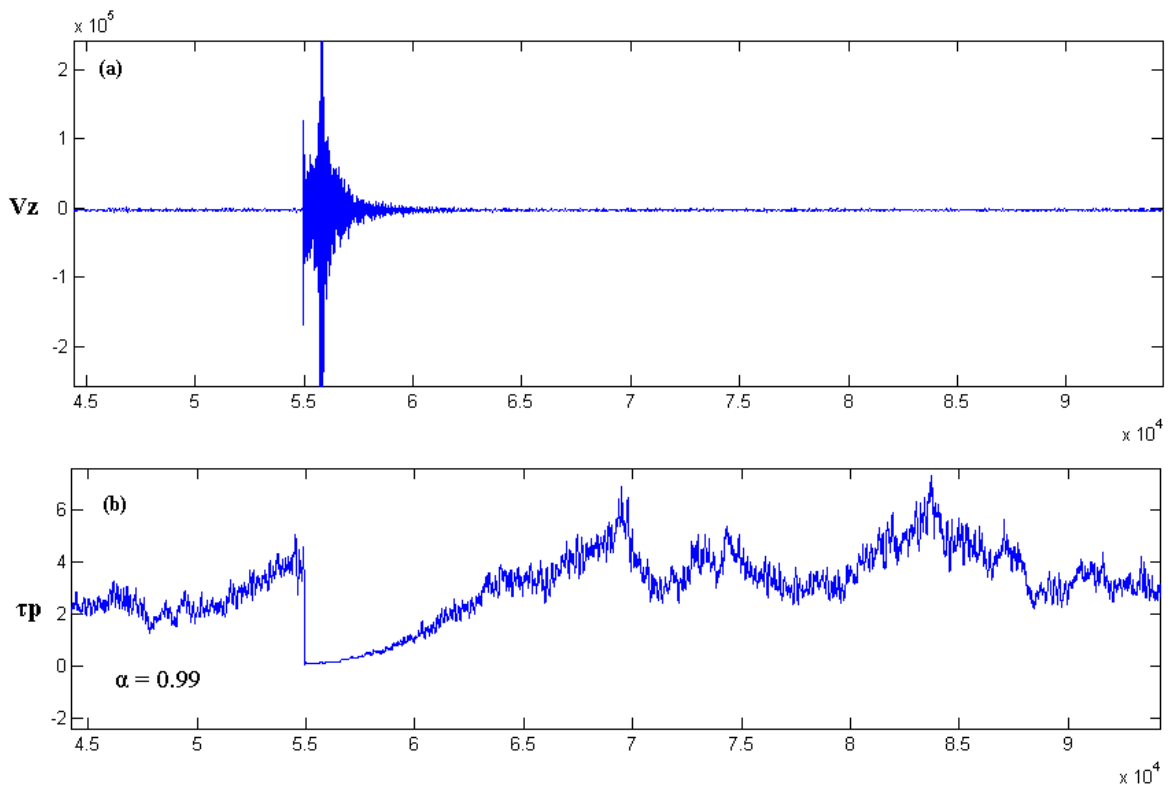
Figure 6.2. Example of τ_p function for one waveform. (a) Vz is the vertical component of velocity record in BODT station. (b) The τ_p function with smoothing constant 0.99

A full automatic code is written in order to calculate the estimated predominant period from the waveform. The program uses a combination of FORTRAN, C-shell and SAC codes. FORTRAN code was written in order to calculate the maximum predominant period in five sec for every station. A SHELL script, using SAC macro, was written in order to select a P-arrival to any station from the HYPO file, pick the waveform from the database, apply low pass filter at 10 Hz and cut the first five seconds of the P arrival times, and finally the FORTRAN code imbedded in the SHELL file estimate the dominant period. Hence, once we have the database and HYPO file ready, we can compute the τ_p^{max} value of the first five seconds for each of the stations in a sequential way without any intervention. Table 6.2 demonstrate the output file that is obtained after the application of data processing described above.

Table 6.2. Example of the output of the maximum predominant estimation

DATE			TIME			STNM	DIST	ML	τ_p^{max} 1sec	τ_p^{max} 2sec	τ_p^{max} 3sec	τ_p^{max} 4sec	τ_p^{max} 5sec
2007	9	23	17	09	18	yer0	71.6	3.9	0.67	0.67	0.67	0.67	0.67
2007	9	23	17	09	18	bodt	16.2	3.9	0.28	0.28	0.28	0.28	0.28
2007	9	23	17	09	18	mlsb	38.1	3.9	1.00	1.00	1.00	1.00	1.00
2007	9	23	17	09	18	dat0	35.4	3.9	0.44	0.44	0.44	0.44	0.44
2007	9	23	17	20	59	yer0	75.5	3.7	0.67	0.67	0.67	0.67	0.67
2007	9	23	17	20	59	bodt	24.1	3.7	0.51	0.51	0.51	0.51	0.51
2007	9	23	17	20	59	mlsb	50.7	3.7	1.88	1.88	1.88	1.88	1.88
2007	9	23	17	20	59	dat0	20.5	3.7	0.41	0.41	0.41	0.41	0.41
2007	10	10	21	27	49	dalt	51.7	3.9	0.30	0.32	0.34	0.34	0.34
2007	10	10	21	27	49	ell0	165	3.9	1.08	1.08	1.08	1.08	1.08
2007	10	10	21	27	49	yer0	37.2	3.9	0.68	0.68	0.68	0.68	0.68
2007	10	10	21	27	49	bodt	71.4	3.9	0.31	0.31	0.31	0.31	0.31
2007	10	10	21	27	49	mlsb	55.7	3.9	0.52	0.52	0.52	0.52	0.52
2007	10	10	21	27	49	blcb	193	3.9	0.22	0.22	0.22	0.22	0.22
2007	10	10	21	27	49	dat0	39.5	3.9	0.49	0.49	0.49	0.49	0.49
2007	10	12	17	06	01	yer0	93.0	4.2	0.57	0.57	0.57	0.57	0.57
2007	10	12	17	06	01	mlsb	107	4.2	0.28	0.28	0.28	0.28	0.28
2007	10	12	17	06	01	blcb	240	4.2	0.25	0.25	0.25	0.25	0.25
2007	11	03	04	24	23	dalt	193	4.9	0.48	0.48	0.48	0.48	0.48
2007	11	03	04	24	23	ell0	306	4.9	0.93	0.93	0.93	0.93	0.93
2007	11	03	04	24	23	bodt	90.0	4.9	0.40	0.40	0.40	0.40	0.40
2007	11	03	04	24	23	mlsb	139	4.9	0.30	0.30	0.30	0.30	0.30
2007	11	03	04	24	23	blcb	205	4.9	0.32	0.32	0.32	0.32	0.32
2007	11	03	04	24	23	dat0	98.4	4.9	0.52	0.52	0.52	0.52	0.52

In Table 6.2, we showed the estimated values of maximum predominant periods in five seconds at individual stations of four different earthquakes.

6.3. Predominant Period – Magnitude Relation

ElarmS methodology calculates τ_p^{max} within four seconds in order to scale with event magnitude, but I calculated τ_p^{max} within five seconds and the results showed that there was not any significant change in τ_p^{max} value after the first one second. Therefore I used the value of τ_p^{max} within one second.

I try to determine a linear relation between τ_p^{max} and magnitude. In order to obtain the best relation I put some restrictions while plotting the scaling relation, to be described below. A MATLAB code was written in order to plot the relation between τ_p^{max} and magnitude, besides determine the best fit relation between them using least squares fitting, and finally calculate the variables of the equation that is used for calculating the magnitude of an event with utilizing its maximum predominant period.

The principle of the restrictions consists of first eliminating very distant recordings when magnitudes are small, and second rejection of those predominant period values which are outside a given acceptable range. The MATLAB code simply reads the output of predominant period estimation file. If the magnitude of the earthquake is smaller than 3.4 then the algorithm eliminates the τ_p^{max} values of the stations according to their distance to the epicenter. In other words, when the magnitude of the event gets smaller, than the distance limit that I use gets smaller too. For example, if the magnitude of an earthquake is 3.0 then the distant limit that I put becomes 56 km, if the magnitude of the event is 2.0 then the distant limit becomes 34 km. If the magnitude of an earthquake is equal and larger than 3.4, I didn't put any distance limit restriction. In both two situations I also did not take into account τ_p^{max} values bigger than one.
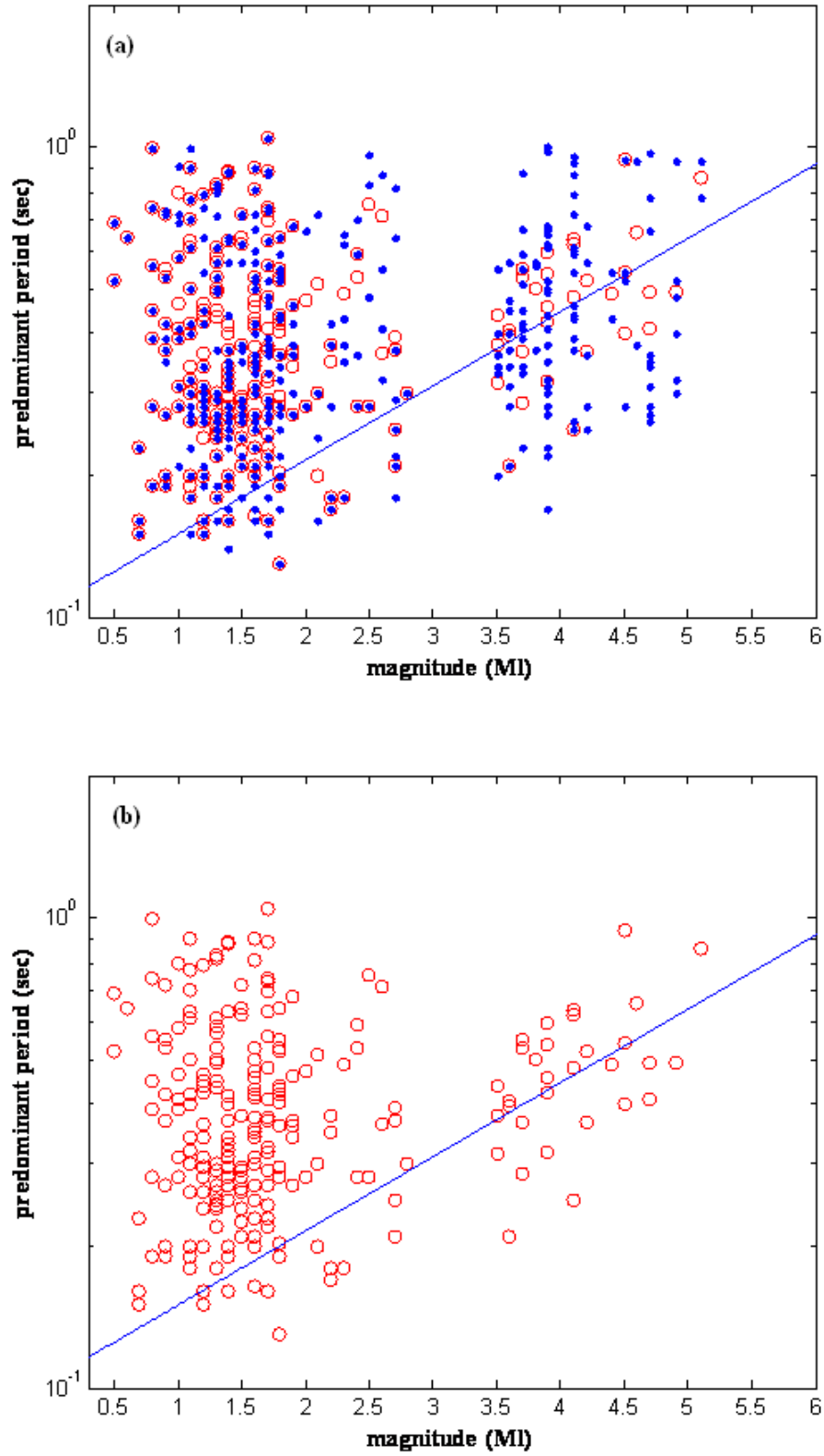
Figure 6.3. Relation between τ_p^{max} and magnitude. Blue line shows the linear fit using events with M>3.5 (see text) (a) shows both individual stations and their averages. (b) shows only average values of τ_p^{max} versus magnitude

Figure 6.3 shows the magnitude versus predominant period relation. Predominant period was measured from the vertical component of broadband velocity sensor. Blue dots indicate maximum predominant period within one second of the P wave arrival low pass filtered at 10 Hz versus local magnitude of the events for individual stations. Red circles indicate magnitude found by averaging all predominant periods for an individual event. The striking outcome of the experiment in Gökova is the observation of the fact that the method works well for earthquakes above the magnitude threshold of 3.0 but fails for smaller ones. In fact the estimated predominant periods for events less than 3.0 shows a very large scattering. One also need to note that for small events there is always less number of stations to take the average due to distance limitation. This also probably one of the reasons to increase the scattering. There is also the problem of having smaller pulse for small earthquakes which present higher uncertainty for period estimation by the method used. The sampling rate may also play an important role in the performance of the algorithm. Note that in the publication related to this method there was never any results given for small events which are below the magnitude 3.0. It is clear that this points needs to be studied further. I therefore continue the analysis by excluding events that are smaller than 3.0. Figure 6.4a shows all period estimates at both individual stations (in blue) and event averaged estimates (in red) for the events larger than 3.0. Figure 6.4b shows the event averaged estimates and I also calculated the standard deviation of the event averaged estimates as 0.12 seconds which was shown in green line. As one would expect the averaged estimates show much less scattering than the individual ones.
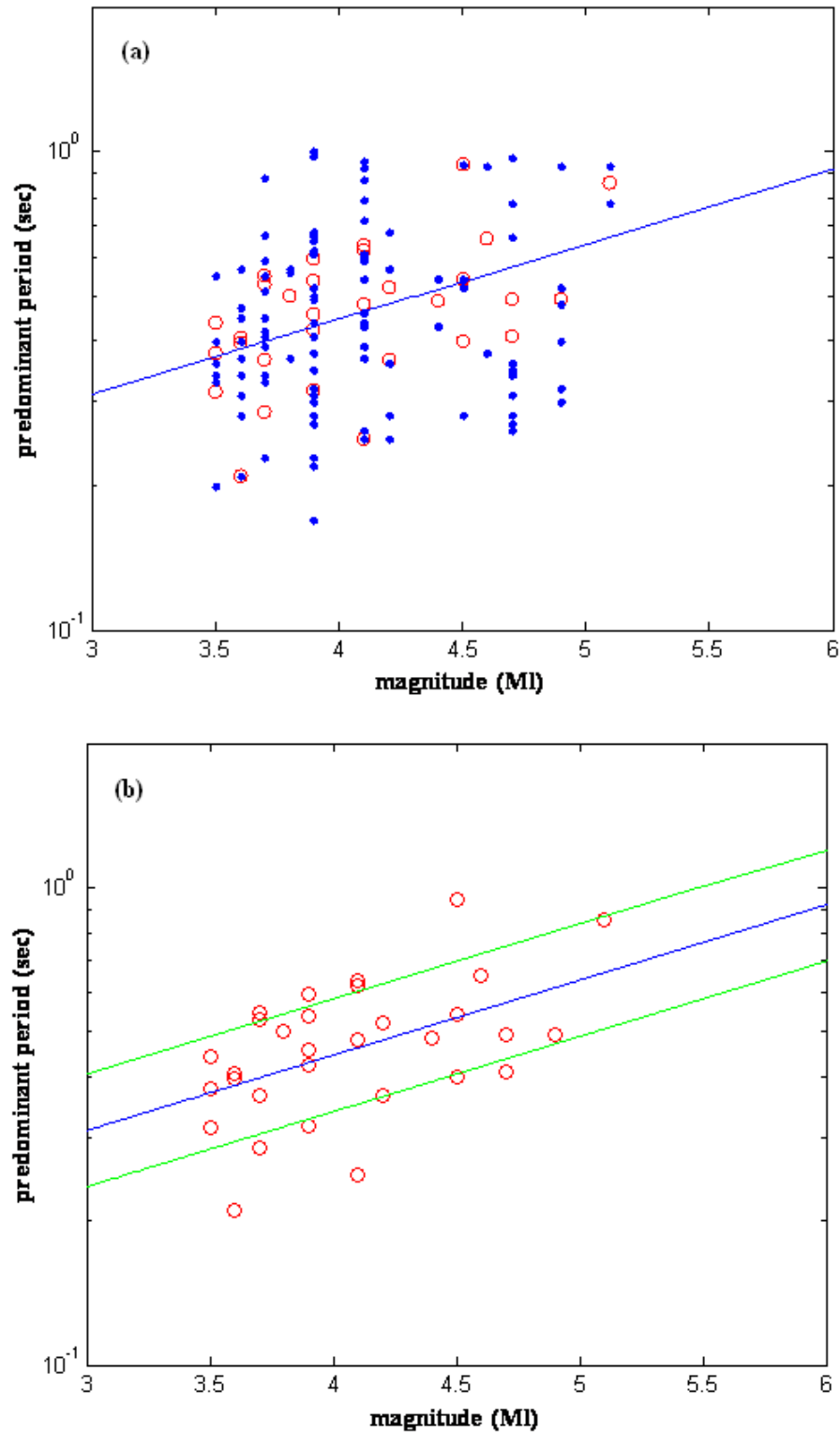
Figure 6.4. Relation between τ_p^{max} and magnitude for earthquakes larger than 3.0. (a) shows both individual stations and their averages. (b) shows only average values of τ_p^{max} versus magnitude for Gökova, Turkey

A least-square fit of Ml on the logarithm of maximum predominant period is obtained by using the averaged periods and gives the following relation

$$Ml = 6.3583log\ (\tau_p{}^{max}) + 6.238 \qquad\qquad (6.4)$$

This relation is used in order to estimate the magnitude of earthquakes. After the first station triggers, ml magnitude is calculated from $\tau_p{}^{max}$, and when second station triggers the same operation is repeated for this new station and the estimate is updated by taking average of the two estimates. As more stations pick the arrivals the estimate is further updated by the additional data.

In the previous chapters we've mentioned that the ElarmS was tested in southern California, Japan and Italy too. Therefore we compare our test results with them. It is interesting to see that there is a perfect matching of our result with those of California and Japan. As far as the linear relation between the period and the magnitude is concerned. In Figure 6.5 the relation between $\tau_p{}^{max}$ and magnitude is showed for southern California, Japan (Allen, 2005) and Italy (Olivieri *et al*., 2008) in a), b) and c), respectively.

Figure 6.6 was prepared using MATLAB program and it shows the relation between $\tau_p{}^{max}$ and magnitude for all four regions: namely Italy, southern California, Japan and Gökova Turkey. All relations, except one from Italy show large similarity with each other, especially Japan and Gökova were perfectly coherent such that they cannot be distinguished in the figure. It is difficult to explain at this stage why the period-magnitude relationship for Italy greatly differs from the three others. Incorporation of wide range of tectonic regimes into the analysis, joint processing of a wide range of seismometers types or possible errors in local magnitude calculation may be among likely explanation of incoherence for Italy.
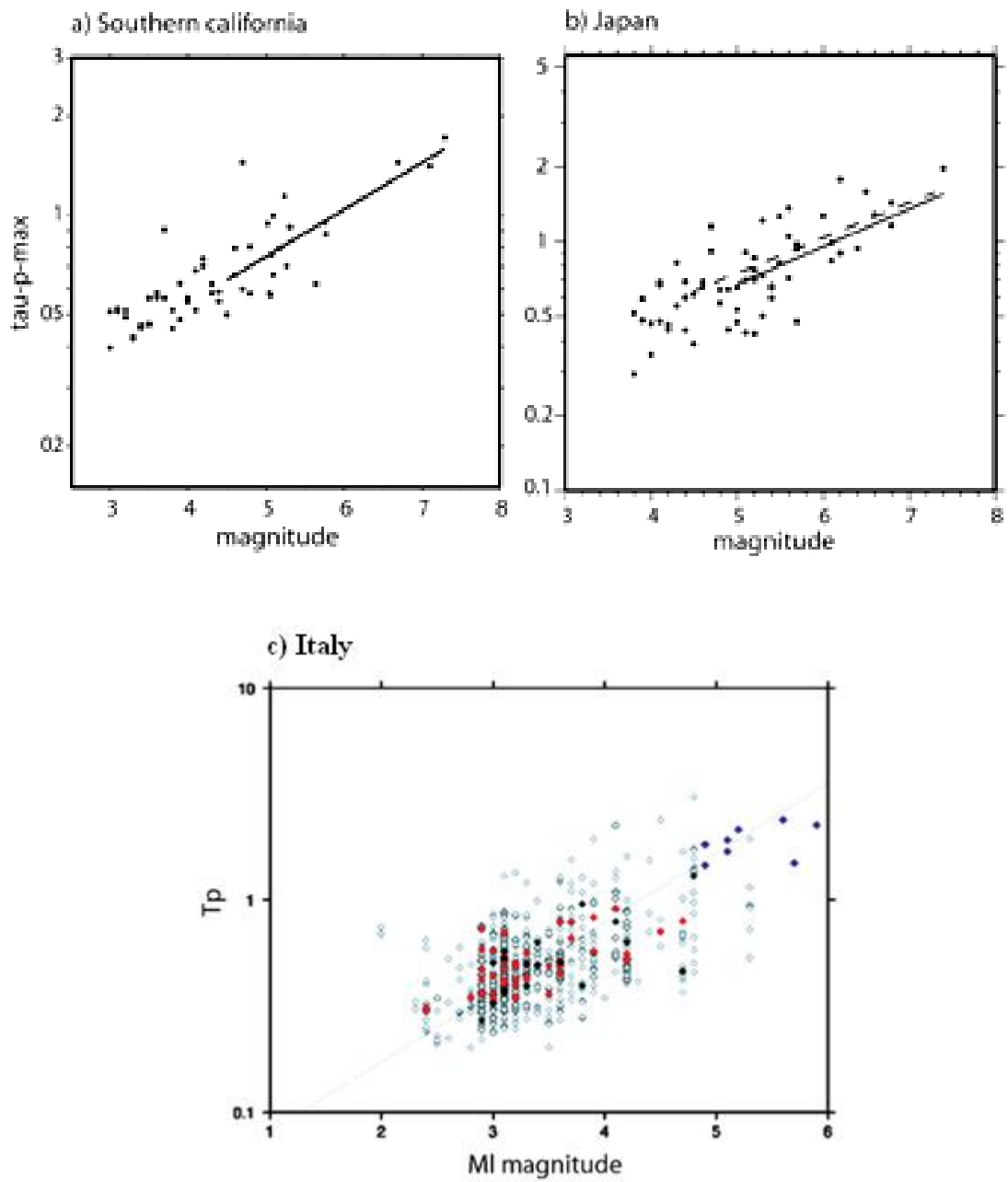
Figure 6.5. Scaling relation between τ_p^{max} and magnitude. Black dots indicate event averages. a) Southern California earthquakes (Allen, 2005) b) Japan earthquakes (Allen, 2005) c) Italy earthquakes (Olivieri *et al*., 2008)
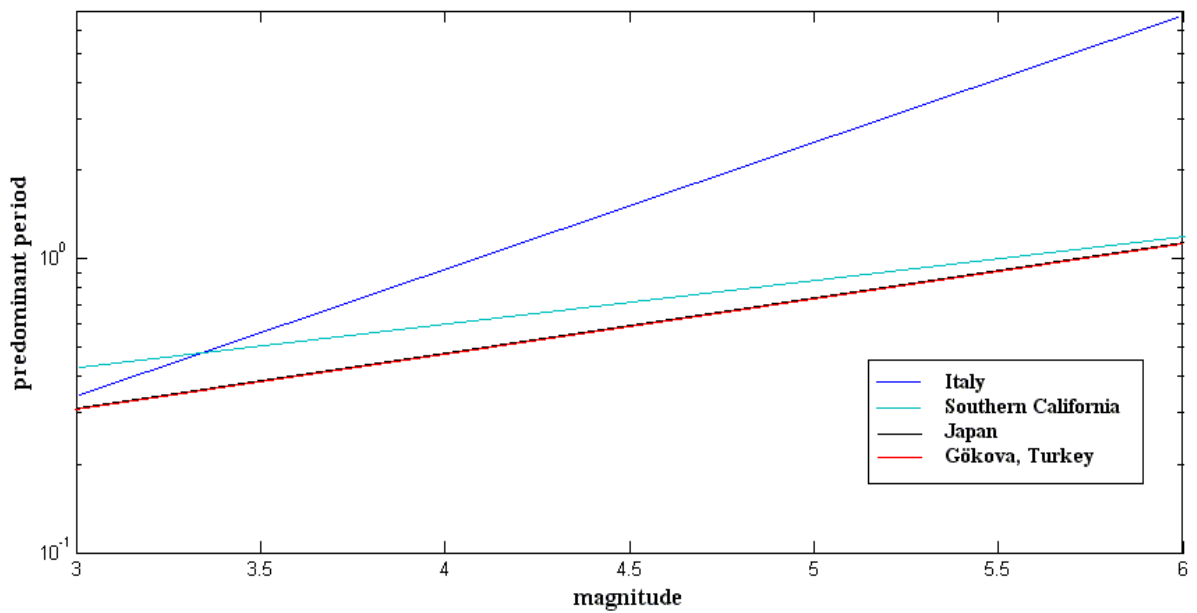
Figure 6.6. Relation between τ_p^{max} and magnitude for four different regions

Figure 6.7 shows the comparison of real Ml magnitudes versus predicted ElarmS magnitude for Gökova, Turkey. Figure 6.8 shows the same for Italy (Olivieri *et al*., 2008). One can detect some differences between the two examples. A perfect comparison is not possible at this stage because the magnitude range covered in this thesis does not cover high end namely M>5.0. This is mainly because the thesis study area is restricted to a small area (Gökova Bay) as compared to the Italian case which covers the whole country.
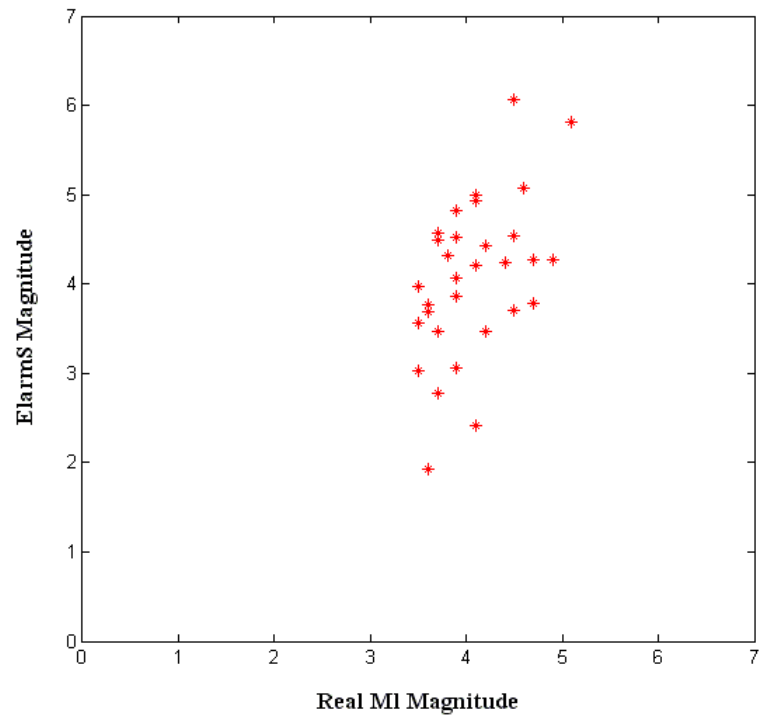
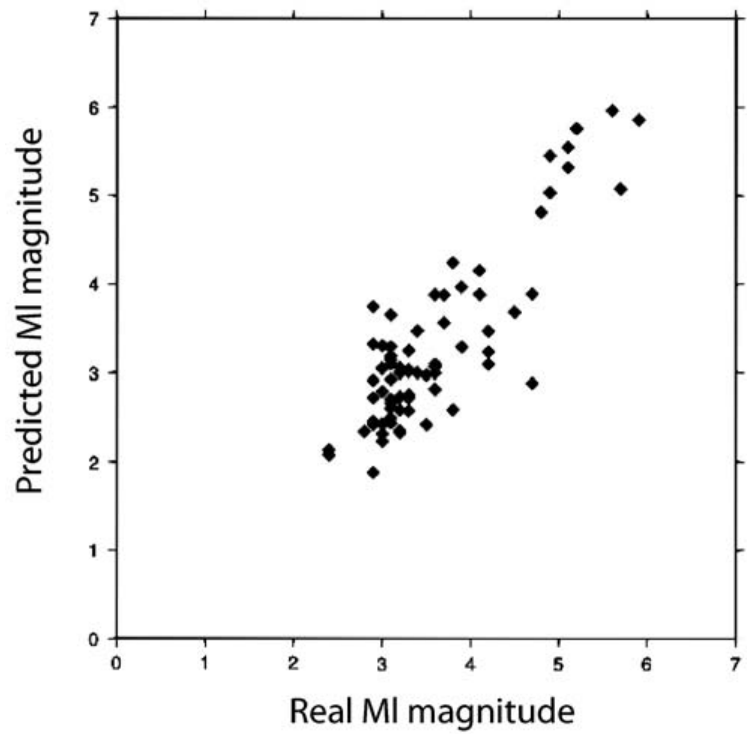Figure 6.7. Real Ml magnitude versus predicted ElarmS magnitude for Gökova, Turkey

Figure 6.8. Real Ml magnitude versus predicted ElarmS magnitude for Italy
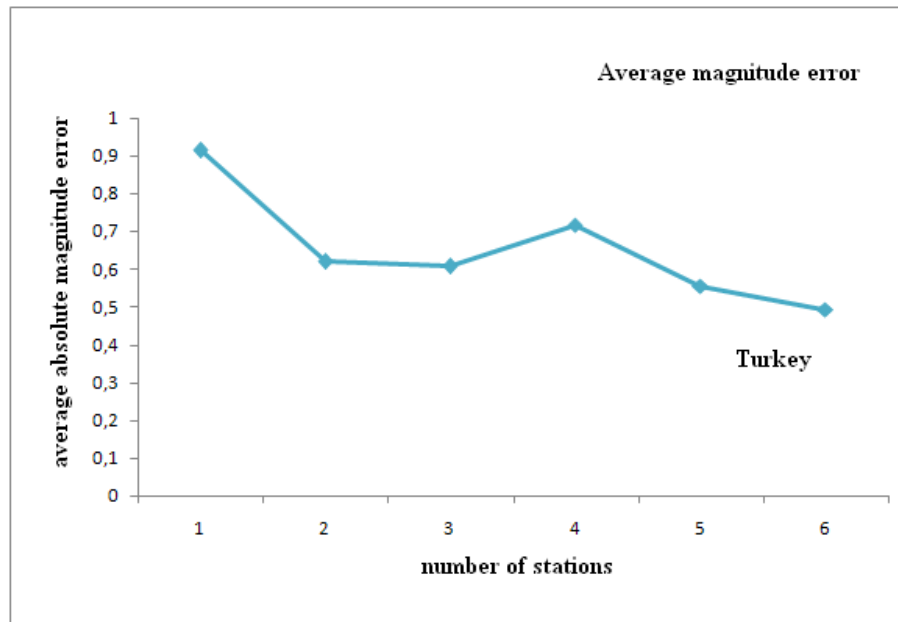
(Olivieri *et al.*, 2008)

Figure 6.9. Average absolute magnitude error as a function of the number of stations providing P-arrivals for Gökova, Turkey
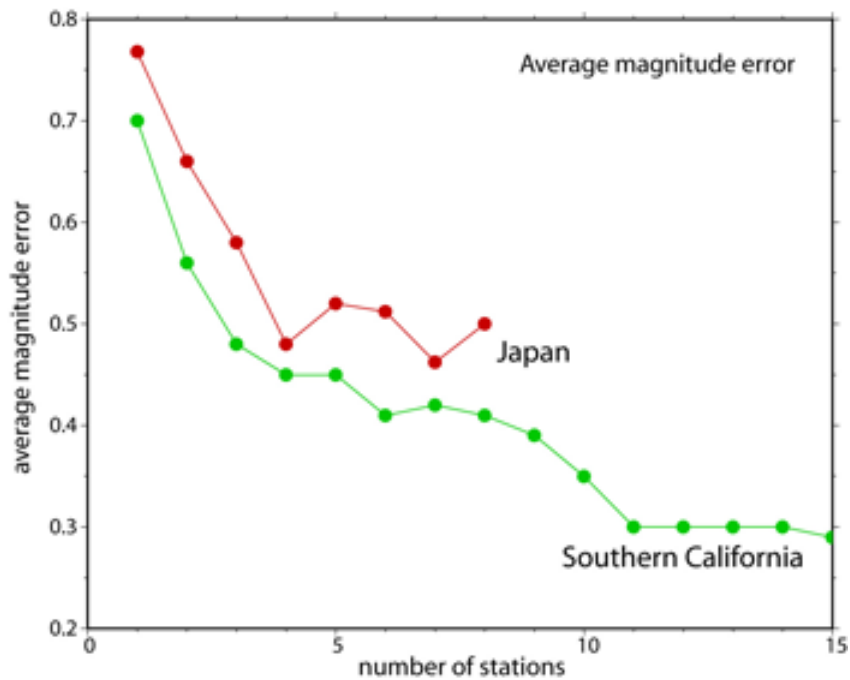

Figure 6.10. Average absolute error in magnitude estimates as a function of the number of stations providing P-wave data for southern California and Japan (Allen, 2005)

The accuracy of magnitude estimation is connected with the number of stations. In other words, the magnitude error decreases when multiple stations are used (Fig. 6.9). While estimating the magnitude of an earthquake with using single station, we used the closest station to the epicenter. Using one station, the average error is about ± 0.9 magnitude units, it drops to approximately ± 0.6 when two stations data available, once six stations data provided the error drops to ± 0.49 magnitude units. The change in the average magnitude error against the number station is shown in Figure 6.9. In Figure 6.10 the same relation is shown for Japan and southern California (Allen, 2005).

6.4. Testing ElarmS with Synthetic Seismogram

The observation that showed the inability of the algorithm for small size events lead me to test the event with synthetic data where it would be possible to check this property with controlled parameters. The method that is used to generate the synthetic waves is the frequency-wavenumber method developed by Bouchon (1981). The method is based on point source simulation in horizontal layered earth model. The approach is based on the wavenumber representation of wave fields and uses the approximation of continuous integrals in time and space by periodicity and discrete summation. The sample we used in this test is the simulated seismogram of the Marmara Sea earthquake occurred on 29th of September 2004. The moment magnitude of the earthquake was given as 4.2 and the epicenter of the earthquake was Çınarcık basin which is located about 10 km southwest of Büyükada (Kalafat and Güneş, 2004).

This earthquake is studied in detail by Seda Yelkenci for her PhD Thesis. All the parameters such as crustal structure, location, distance to the station, fault plane solution and fault area were taken from that study. The seismic recording at ISK station in NEMC was used for the testing and the distance to the epicentre was 30 km.

In order to obtain different magnitude sizes, the rupture area and slip value were changed. The slip values were calculated using relationship between fault length versus moment (Scholz *et al*., 1986). I generated 16 seismograms with magnitudes range between 3.4 and 5.9. Figure 6.11 shows four generated synthetic seismograms. Table 6.3 shows the calculated Ml and predominant period values of the synthetic data set.

Table 6.3. Calculated Ml and τ_p^{max} values of synthetic data set

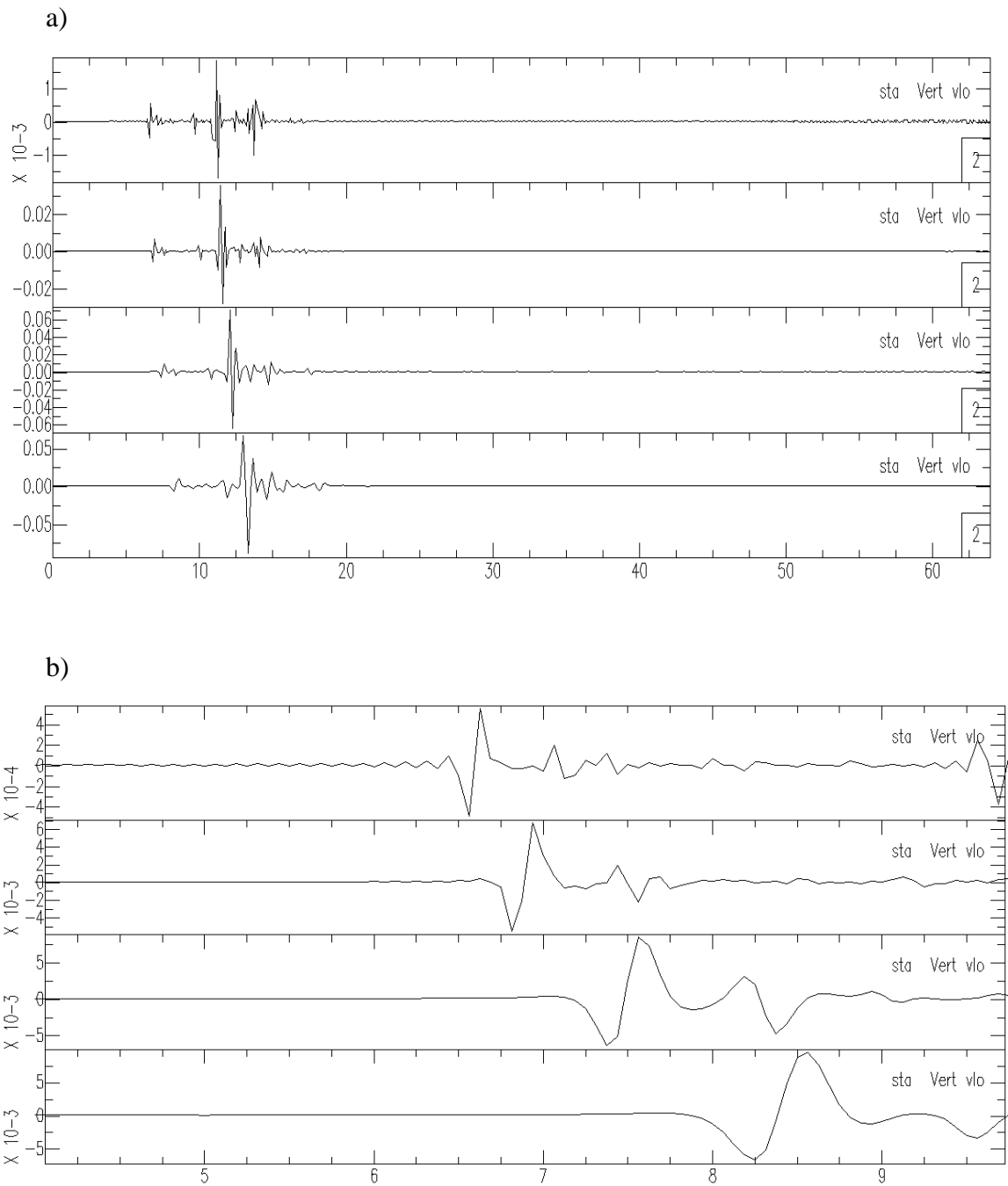| Rupture Area (km^2)	Ml	τ_p^{max} 1 sec
1	3.4	0.24
1.5	3.8	0.24
2.25	3.9	0.24
4.84	4.4	0.25
9.6	4.7	0.27
12	4.8	0.27
15	5.0	0.30
20	5.1	0.46
24	5.2	0.38
25	5.2	0.57
30	5.4	0.32
50	5.7	0.31
60	5.6	0.75
70	5.7	0.75
100	5.8	0.83
200	5.9	1.22

a)

b)

Figure 6.11. Examples of generated seismograms. a) shows synthetic data with magnitudes 3.9, 5.2, 5.7 and 5.9, respectively b) shows the same traces with an enlarged mode
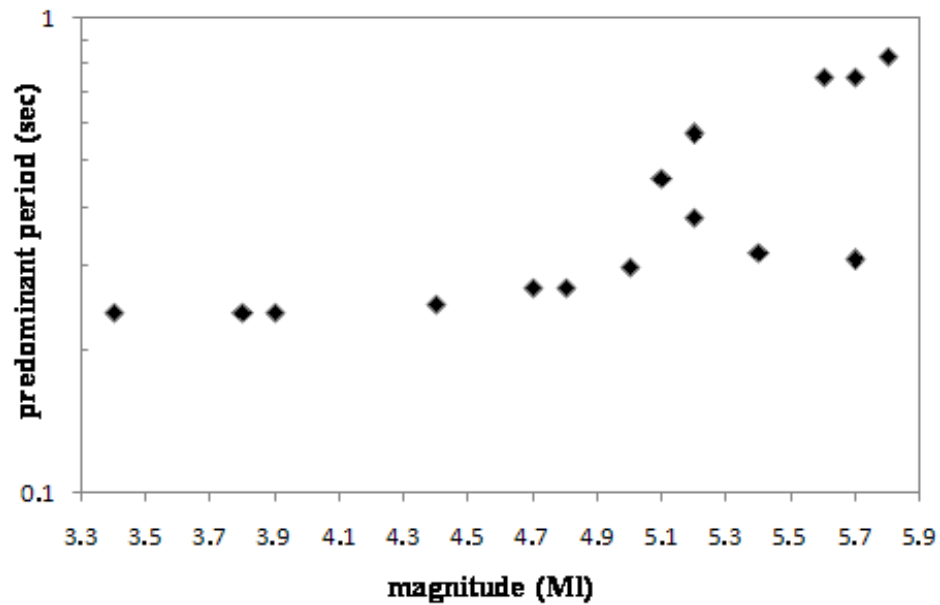
Figure 6.12. Relation between τ_p^{max} and magnitude using synthetic data

Figure 6.12 shows clearly that the predominant period increases as the magnitude of the synthetic event gets larger. However one can notice the peculiar behaviour that was also observed in real data. This is fact that as the magnitude gets smaller, in other words as the pulse width of P-arrival decreases the estimates of dominant period become inefficient. This may be due to inefficiency of the estimation algorithm that is used and which is based on an approximate AR modelling of the time series. This method works may not work well in extreme situation where the noise level is zero as in the case of synthetic modelling. The sampling may also play a critical role in this estimation process. These points need further definitely further deeper studies. For larger magnitude however, in particular for M> 4.0 the algorithm becomes efficient. Few spurious estimates were also observed for some examples of large magnitude. These are situations where the same magnitude is obtained by using different shapes of rupture areas in generating the synthetics. This is also a point of further investigation.

7. CONCLUSIONS

ElarmS methodology uses the frequency content of the first few seconds of P-arrival and determines the magnitude of the event using predominant period of the seismic signal in few seconds from the vertical component of the seismometer. The key utility in this method is to predict the magnitude of an earthquake without the knowledge of the location of the event. I have tested ElarmS using offline on a data set of 242 earthquakes with local magnitudes range from 0.5 to 5.1. Thirty one of them with magnitudes 3.5 or larger, the rest of them were smaller than 3.0. Using the scaling relation between $\tau_p^{\ max}$ estimated in one sec and Richter magnitude, I observed that events with magnitudes smaller than 3.0 did not showed clear relation between $\tau_p^{\ max}$ and magnitude, on the other hand, events with magnitude larger than 3.5 show a logarithmic relationship.

It is known that the seismic energy disperse with distance and this attenuation mostly occurs at higher frequencies. Correspondingly, due to the short period and low amplitude content of small earthquakes, the seismic energy attenuates more quickly as the distance to the recording station increases. Therefore when a small event occurs far away from the stations the high frequency content is possibly attenuated when it reaches the station and its frequency cannot be estimated properly. That is how we explain the large scatter between τ_p^{max} and magnitude for small earthquakes. The disadvantage of mis-estimating small earthquakes would cause serious problems such as issuing false alarms to the public. In order to fix this problem seismic stations which are very close to earthquake sources should be installed.

On the other hand, I observed that the system was successful for events larger than 3.5. The value of the best-fit slope for Gökova, Turkey coincided perfectly with Japan and Southern California. Especially I observed that Japan and Gökova were totally coherent with each other, besides Italy was dramatically different from the other ones. The remarkable point here was the great similarity between Japan and Gökova, although the regions are differing from each other in terms of faulting mechanisms. In the previous studies, namely Japan and California, the ElarmS methodology was tested with earthquakes generated by strike-slip and reverse fault systems but in Gökova, earthquakes

are generated by normal faulting. Hence it is obvious that ElarmS methodology is feasible for different fault types.

I observed that the accuracy of the magnitude estimates from $\tau_p{}^{max}$ observations increases with the number of stations. When a single $\tau_p{}^{max}$ value from the closest station is used, average magnitude error is ±0.91, when two stations data available the error decreases to ±0.62, when six stations are used the average magnitude error drops to ±⬚0.49. However, decrease of magnitude errors with the number of stations is not guaranteed, particularly for small earthquakes where it is the important to measure $\tau_p{}^{max}$ from closest stations to the epicentre in order to avoid signal losses. For southern California it was mentioned that when ten closest stations were used the average magnitude error was calculated ±0.35. This example indicates that the presence of dense seismic stations near active fault zones is very important for the purpose of rapid earthquake detection. So increasing the number of stations seems to be the best solution for improving the magnitude estimation of small events. On the other hand, an associated problem exists when recording very large events from close distances. In this situation we need to use strong motion seismometers to avoid saturation problem.

Due to the inability of the ElarmS method for earthquakes with small size, I tested the system with synthetic data in order to understand the behaviour of the method with controlled parameters. I have generated 16 seismograms, using frequency-wavenumber method developed by Bouchon (1981), with magnitudes range from 3.9 to 5.9 and observed that the predominant period estimated in one second increases as the magnitude of the events gets larger, similar to what was observed in real data. For synthetic events with magnitudes smaller than 4.0 the change in the predominant period is very slow. This behaviour of the algorithm might depend on two reasons. Firstly, for small magnitude events, the estimation of predominant period becomes inefficient as the pulse width of the P arrival decreases. Secondly, the algorithm is based on an approximate AR modelling of the time series and this method may not work on synthetic seismograms where the noise is zero. This particular behaviour needs to be investigated in further detail.

The keystone of ElarmS methodology is to predict the magnitude of an earthquake with predominant period derived from the initial seconds of a seismogram. The idea behind this is the scaling relation between the initial phases of earthquake rupture and the final size of the earthquake. As Nielsen and Madariaga (2003) mentioned the energy concentration differs when the fracture propagates in large crack or in small crack. Furthermore fractures which have longer rise-time are going to generate low frequencies and this will lead us to observe large dominant period in the early phases of the recordings as an indicator of a large energy concentration which controls the advancement of the fracture. As a consequence, earthquakes with large dominant periods are the indicator of large energy flow, and large energy flow is the indicator of large crack opening, large cracks are in turn the indicator of large magnitude earthquakes.

In conclusion, I tested ElarmS only for Gökova region with earthquakes occurred for the past four years. In order to obtain more comprehensive results the study region can be expanded to whole Turkey. The estimation algorithm for the dominant period needs to be investigated in more detail and possibly be improved. The performance of the method is expected to improve parallel to the observation network (more stations, higher sampling rate, *etc*).

REFERENCES

Aktar, M., H. Karabulut, D. Childs, A. Mutlu, M. Ergin, A. Yörük, V. Gecgel, F. Bulut, T. Kaya, 2006, *Active Faults and Present Seismic Activity in Gökova Bay*, TÜBİTAK Report, January, No: 104Y336.

Allen, R. M., and H. Kanamori, 2003, "The Potential for Earthquake Early Warning in Southern California", *Science,* 300, 786-789.

Allen, R. M., 2005, "*ElarmS Methodology*", http:// www.elarms.org/info/Methodology May05/MethodologyMay05.php

Allen, R.M., 2007, "The ElarmS Earthquake Early Warning Methodology and Application across California", in P. Gasparini, G. Manfredi and J. Zschau (eds.), *Earthquake Early Warning Systems*, Springer Berlin Heidelberg Publisher, New York.

Allen, R. M., 2009, *Earthquake Early Warning in the United States,* Seismological Laboratory, UC Berkeley, http://www.elarms.org/EEWinUS.pdf

Allen, R., 2010a, *Earthquake Early Warning in the United States*, Seismological Laboratory, UC Berkeley, http://www.elarms.org/index.php

Allen, R., 2010b, *Earthquake Early Warning in the United States*, Seismological Laboratory, UC Berkeley, http://www.elarms.org/front/eewGlobal.php

Ambraseys, N. N. and C. Finkel, 1995, "*The Seismicity of Turkey and Adjacent Areas, A Historical Review, 1500-1800*", Eren Publishers.

Bouchon, M., 1981, "A Simple Method to Calculate Green's Functions for Elastic Layered Media", *Bulletin of the Seismological Society of America*, Vol. 71, pp.959–971.

Böse, M., M. Erdik and F. Wenzel, 2007, "A New Approach to Earthquake Early Warning", in P. Gasparini, G. Manfredi and J. Zschau (eds.), *Earthquake Early Warning Systems*, Springer Berlin Heidelberg Publisher, New York.

Brown, H. M. and R. M. Allen, 2009, "Testing ElarmS in Japan", *Seismological Research Letters*, Vol. 80, No. 5, pp. 727-739, September/October.

Erdik, M., 2000, "*Report on 1999 Kocaeli and Duzce (Turkey) Earthquakes*", http://www.koeri.boun.edu.tr/depremmuh/eqspecials/kocaeli/Kocaelireport.pdf

Ersoy, Ş., 1991, "Stratigraphy and Tectonics of the Datça (Muğla) Peninsula", *Geological Bulletin of Turkey*, V. 34, 1-14, August.

Felzer, K., 2006, "*Calculating the Gutenberg-Richter b Value*", http://pasadena. wr.usgs.gov/ office/ kfelzer/AGU2006Talk.pdf, USGS

Gasparini, P., G. Manfredi and J. Zschau, 2007, "*Earthquake Early Warning Systems*", Springer Berlin Heidelberg Publisher, New York.

Guidoboni, E. and A. Comastri, 2005, "Catalogue of Earthquakes and Tsunamis in the Mediterranean Area from the 11th to the 15th Century", *Istituto Nazionale di Geofisica e Vulcanologia*, p. 1027.

Havskov, J. and L. Ottemöller, 2005, SEISAN: The Earthquake Analysis Software For Windows, SOLARIS, UNIX and MACOSX, Version 8.1, August.

Ionescu, C., M. Böse, F. Wenzel, A. Marmureanu, A. Grigore and G. Marmureanu, 2007, "An Early Warning System for Deep Vrancea (Romania) Earthquakes", in P. Gasparini, G. Manfredi and J. Zschau (eds.), *Earthquake Early Warning Systems*, Springer Berlin Heidelberg Publisher, New York.

Kalafat, D., and Y. Güneş, 2004, "*29 September 2004 Marmara Sea Earthquake*", http://www.koeri.boun.edu.tr/sismo/default.htm

Kalafat, D., Y. Güneş, K. Kekovalı and M. Berberoğlu, 2004, "*Earthquake Activity of the Gulf of Gökova*", B.U., Kandilli Observatory & ERI, National Earthquake Monitoring Center, www.emsc-csem.org/Doc/Gokova_0804.pdf

Kalafat, D., C. Zülfikar, E. Vuran and Y. Kamer, 2010, "*08 March 2010 Başyurt-Karakoçan (Elazığ) Earthquake*", http://www.koeri.boun.edu.tr/sismo/default.htm

Nakamura, Y., B. E. Tucker, 1988," Earthquake Warning System for Japan Railways", Bullet Trains: Implications for Disaster Prevention in California, *Earthquakes and Volcanoes,* Vol.20, 140-155.

Nakamura, Y., 1988, "On the Urgent Earthquake Detection and Alarm System (UREDAS)", *Proceedings of Ninth World Conference on Earthquake Engineering,* VII, 673-678.

Nakamura, Y., 2004, "UrEDAS, Urgent Earthquake Detection and Alarm System, Now and Future", *13th World Conference on Earthquake Engineering*, Canada, 1-6 August 2004, pp. 908.

Olivieri, M., R. M. Allen, and G. Wurman, 2008, "The Potential for Earthquake Early Warning in Italy Using ElarmS", *Bulletin of the Seismological Society of America*, Vol. 98, No. 1, pp. 495–503.

PASSCAL, 2009, *PQL II-Program for Viewing Data*, http:// www.passcal.nmt.edu/content /pql-ii-program-viewing-data

Scholz, C. H., C. A. Aviles and S. G. Wesnousky, 1986, "Scaling Differences between Large Interplate and Intraplate Earthquakes", *Bulletin of the Seismological Society of America*, Vol. 76, pp. 65-70.

Soysal, H., S. Sipahioğlu, D. Kolçak and Y. Altınok, 1981, *Historical Earthquake Catalogue of Turkey and Surrounding Area (2100 B.C. – 1900 A.D.)*, Technical Report, TUBİTAK, No: TBAG-341.

Tan, O., M. C. Tapırdamaz and A. Yörük, 2008, "The Earthquake Catalogues for Turkey", *Turkish Journal of Earth Sciences*, Vol. 17, pp. 405-418.

USGS, 1995, http://countrystudies.us/turkey/20.htm

Uluğ, A., N. Kaşer and M. Duman, 2005, "The Gulf of Gökova and Environment Anatomy and Its Earthquakes", *The Fifth National Symposium of Shore Engineering*, Antalya, 5 May 2005, http://www.e-kutuphane.imo.org.tr/pdf/10644.pdf

Uluğ, A., M. Duman, Ş. Ersoy, E. Özel and M. Avcı, 2005, "Late Quaternary Sea-Level Change, Sedimentation and Neotectonics of the Gulf of Gökova: Southeastern Aegean Sea", *Marine Geology*, 221, 381– 395.

Uluğ, A. and N. Kaşer, 2007, "The Seismicity and Active Faulting Around the Gulf of Gökova in the Southwestren Turkey", *Rapp. Comm. int. Mer Médit*., 38.

Weber, E., G. Iannaccone, A. Zollo, A. Bobbio, L. Cantore, M. Corciulo, V. Covertito, M. Di Crosta, L. Elia, A. Emolo, C. Martino, A. Romeo and C. Satriano, 2007, "Development and Testing of an Advanced Monitoring Infrastructure (ISNet) for Seismic Early-warning Applications in the Campania Region of Southern Italy", in P. Gasparini, G. Manfredi and J. Zschau (eds.), *Earthquake Early Warning Systems*, Springer Berlin Heidelberg Publisher, New York.

Wu, Y. -M. and T. –L. Teng, 2002, "A Virtual Subnetwork Approach to Earthquake Early Warning"*, Bulletin of the Seismological Society of America*, Vol. 92, No. 5, pp. 2008–2018.

Yeats, R. S., K. Sieh and R. C. Allen, 1997, *The Geology of Earthquakes*, Oxford University Press, New York.

REFERENCES NOT CITED

Nielsen, S., 2007, "Can Earthquake Size be Controlled by the Initial Seconds of Rupture ?", in P. Gasparini, G. Manfredi and J. Zschau (eds.), *Earthquake Early Warning Systems*, Springer Berlin Heidelberg Publisher, New York.